Received: 14 January 2020 | Revised: 1 July 2020 | Accepted: 20 July 2020

DOI: 10.1111/ejn.14926

RESEARCH REPORT

EJN European Journal of Neuroscience FENS WILEY

Evidence of inverted gravity-driven variation in predictive sensorimotor function

Andrew Isaac Meso[1,2,3] | **Robert L. De Vai**[3] | **Ashakee Mahabeer**[3] | **Peter J. Hills**[3]

[1]Neuroimaging Department, Institute of Psychiatry, Psychology and Neuroscience, King's College London, London, UK

[2]Institut de Neuroscience de la Timone, Team Invibe, CNRS & Aix-Marseille Université, Marseille, 13005, France

[3]Psychology & Interdisciplinary Neuroscience Group, Bournemouth University, Poole, UK

Correspondence
Andrew Isaac Meso, Neuroimaging Department, Institute of Psychiatry, Psychology and Neuroscience, King's College London, London, UK.
Email: andrew.meso@kcl.ac.uk

Funding information
Bournemouth University

Abstract

We move our eyes to place the fovea into the part of a viewed scene currently of interest. Recent evidence suggests that each human has signature patterns of eye movements like handwriting which depend on their sensitivity, allocation of attention and experience. Use of implicit knowledge of how earth's gravity influences object motion has been shown to aid dynamic perception. We used a projected ball-tracking task with a plain background offering no context cues to probe the effect of acquired experience about physical laws of gravitation on performance differences of 44 participants under a simulated gravity and an atypical (upward) antigravity condition. Performance measured by the unsigned difference between instantaneous eye and stimulus positions (RMSE) was consistently worse in the antigravity condition. In the vertical RMSE, participants took about 200 ms longer to improve to the best performance for antigravity compared to gravity trials. The antigravity condition produced a divergence of individual performance which was correlated with levels of questionnaire-based quantified traits of schizotypy but not control traits. Grouping participants by high or low traits revealed a negative relationship between schizotypy trait level and both initiation and maintenance of tracking, a result consistent with trait-related impoverished sensory prediction. The findings confirm for the first time that where cues enabling exact estimation of acceleration are unavailable, knowledge of gravity contributes to dynamic prediction improving motion processing. With acceleration expectations violated, we demonstrate that antigravity tracking could act as a multivariate diagnostic window into predictive brain function.

KEYWORDS

diagnostics, eye movements, gravity, prediction, schizotypy

Abbreviations: BAI, Beck Anxiety Inventory; FEF, frontal eye fields; GHQ, 12-item General Health Questionnaire; MT, middle temporal visual motion area; PCA, principal component analysis; RMSE, root-mean-square (position tracking) error; SC, superior colliculus; SPQ, Schizotypal Personality Questionnaire.

Editor by Dr. Edmund Lalor

1 | INTRODUCTION

Eye movements are critical for vision both because of the limited size of the section of the retina in which we can see at high resolution and because eliminating movements eventually results in visual fading (Martinez-Conde, Otero-Millan, & Macknik, 2013; Yarbus, 1967). A key role of the visual system is to continuously place and maintain the fovea where it needs to be. To this end, humans use a repertoire of functional movements which include saccades with their ballistic dynamics, smooth tracking and small tremors (Rucci & Victor, 2015). These movements have been studied extensively in paradigms which have helped isolate their characteristics and suggested in a range of contexts that the ocular motor system is a useful window into brain function (Bueno, Sato, & Hornberger, 2019; Freedman & Foxe, 2018; Kowler, 2011; Spering & Montagnini, 2011).

A recent large cohort study looked at performance metrics for classic computer-based eye-tracking tasks involving pro-saccades (towards a target), antisaccades (away from a target) and horizontal smooth pursuit along a linear trajectory (Bargary et al., 2017). The study computed a 21-measurement representation or vector of each individual's eye movement biometrics. When ten per cent of participants were retested, it was found that data from the second session remained uniquely identifiable within the initial bank of 1,000+ individuals. The biometrics therefore captured participants' unique ocular motor signatures. With a better theoretical understanding of the relationships between the components of such biometrics, the roles played by the separate but interconnected sensorimotor networks of brain regions such as striate and extra-striate visual cortex, middle temporal visual motion area (MT), the frontal eye fields (FEF) and the superior colliculus (SC) in generating finely controlled eye movements might be more distinctly isolated and understood (Bueno et al., 2019; Freedman & Foxe, 2018; Masson & Perrinet, 2012).

Smooth pursuit is a skilled movement which improves during development, aided by experience of constantly tracking objects around us. In children, it has been shown to improve with maturity with later development in the vertical direction compared to the horizontal (Ingster-Moati et al., 2009). This difference could reflect a longer time course of accumulating the experience of acceleration due to gravity or result from a biological difference in the neural representation of the vertical and horizontal axes, for example, within the SC (Krauzlis, 2003) and other oculomotor structures (Johannesson, Tagu, & Kristjansson, 2018). A study with limited participants looking at direction anisotropies during smooth pursuit in adults found that individuals were generally better at horizontal than vertical pursuit, but there was no measurable difference between up and down, though the study did not use accelerating stimuli (Rottach et al., 1996). Within studies looking across a broader adult lifespan, asymmetries have been identified in saccade task performance between upward and downward directions of pro-saccades (Bonnet et al., 2013). Differences were not seen for antisaccades and were found to be much more prominent than left–right asymmetries. The latter are sometimes attributed to experience effects of reading in cultures which write from left to right. Within the smooth pursuit data collected by Bargary et al. (2017), they identified the measures of catch-up saccades and root-mean-square errors (RMSE; performance measure based on the unsigned difference between eye position and target stimulus position) as metrics which showed broad distributions of individual differences in performance.

An aspiration of the current work was to use more ecologically valid visual stimulation where saccades and pursuit operate in conjunction to serve performance and their combined effect could be studied (Orban de Xivry & Lefevre, 2007). Linear trajectories typically investigated can successfully isolate smooth tracking from saccades, but such a configuration remains ecologically unlikely. In contrast, it has been found that curved pursuit trajectories can introduce larger catch-up saccades and delays of up to 300 ms from onset before pursuit matches the tracked motion (Ross, Goettker, Schutz, Braun, & Gegenfurtner, 2017). In tracking tasks with blanked trajectories, it was found that motion had to be tracked for up to 500 ms before acceleration could be incorporated into extrapolated motion estimates (Bennett, Orban de Xivry, Barnes, & Lefevre, 2007). We probed the extent to which tracking could be attributed to learned experience of the physical laws of gravity governing dynamic natural scenes. Humans typically find estimating arbitrary accelerations difficult (Werkhoven, Snippe, & Toet, 1992) but have been shown to be sensitive to accelerations due to gravity in dynamic tasks involving interception (Brenner et al., 2016; Mijatovic, La Scaleia, Mercuri, Lacquaniti, & Zago, 2014). Direct judgements of vertical acceleration due to gravity have also been shown to be possible, but with individual variability in the thresholds of 3%–50% of *g* (Kim & Spelke, 1992) or 13%–30% of *g* (Jorges, Hagenfeld, & Lopez-Moliner, 2018) depending on the tasks. A recent review discussed evidence (Jorges & Lopez-Moliner, 2017) that gravity-dependent estimation may strongly rely on multisensory integration with an assumption of downward acceleration. There is evidence that the otolith system in the inner ear which is sensitive to gravity provides a vertical reference frame which then influences aesthetic perception and numeric decision-making (Gallagher, Arshad, & Ferre, 2019; Gallagher & Ferre, 2018). Most of the research on visual processing of gravity has additionally assumed that internal models of gravity require pictorial cues which aid in the calibration or estimation of the value of *g* (Zago, McIntyre, Senot, & Lacquaniti, 2009). This is because for any viewed object, its acceleration on the retina scales linearly with the

distance from the viewer and the expected retinal acceleration due to gravity needed for fast prediction can be estimated from the target object size and depth. Indeed, contextual information is seen to influence estimation for catching of both familiar and unfamiliar objects (Hosking & Crassini, 2010) and trajectory discrimination of balls of variable sizes (Jorges et al., 2018). There are therefore outstanding questions about the extent to which sensitivity to gravity can be maintained when these contextual visual cues are impoverished. These are particularly pertinent as processing potentially complex contextual cues may be costly for an organism faced with a hostile dynamic environment.

For a simple moving dot stimulus without visual cues to object depth and expected retinal acceleration, we considered what measurable consequences experienced might engender. Gravity acts downwards for most of us over the lifespan providing a strong physical constraint on naturalistic object motions. The value of g is almost constant across the globe varying by less than 0.5% ranging from 9.78 m/s^2 at the equator to 9.83 m/s^2 at the poles (Young, Freedman, & Ford). We develop a projected bouncing ball task in which a small circle moves along a plain grey background with a constant horizontal speed and variable initial and subsequent vertical speed (see Figure 1a). Curvature of the trajectory along a parabola is governed by a vertical acceleration due to gravity (or upward antigravity), and there are some abrupt speed changes due to collisions with virtual walls on either side of the task space which occur after the half a second we consider in the current work. We compute a simple time-varying performance measure (dynamic RMSE) to compare our conditions and contrast individual differences in tracking across what we expect to be a highly learned (gravity) against an unfamiliar (antigravity) acceleration condition. We probe what this can reveal about how individuals typically and atypically accomplish dynamic visual processing.

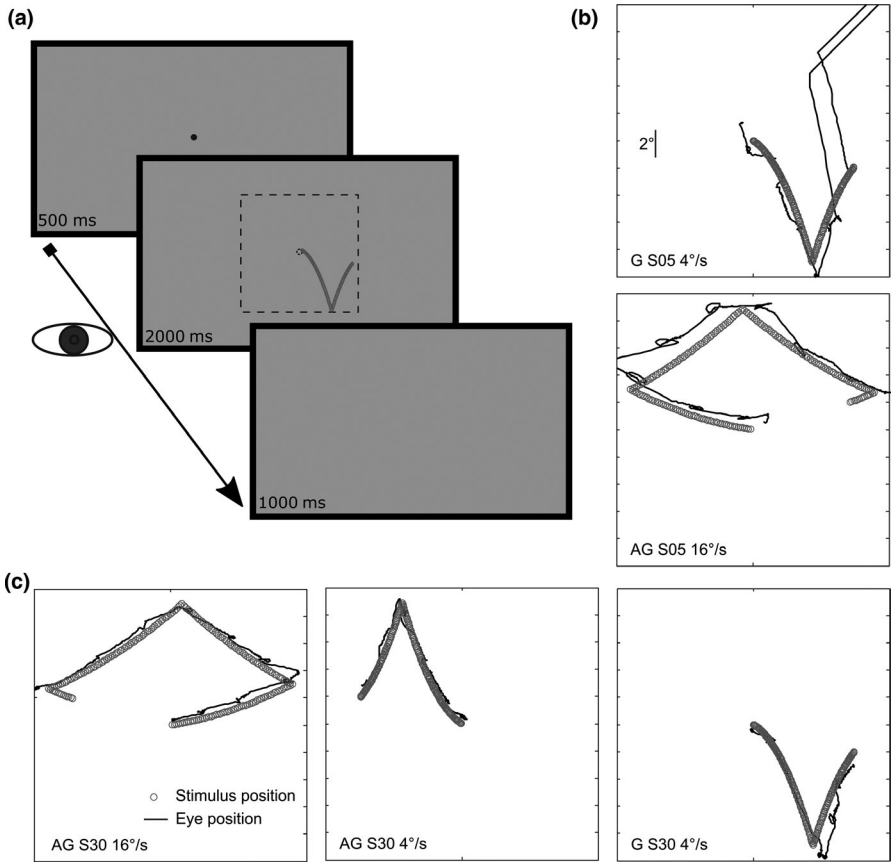

FIGURE 1 Tracking task schematic and example traces. (a) Illustration of task sequence in three screens showing initial 500 ms grey screen with fixation, then the 2-s stimulus presentation for the 4°/s target under gravity moving within the virtual stimulus square in the dashed lines (note: the dashed line is not seen by participants) and finally the post-stimulus 1 s grey screen. After the grey screen, a button press initiates a new fixation and trial. (b) Two examples of tracked stimuli for participant S05 under gravity at 4°/s (top) and under antigravity at 4°/s (bottom). The grey circles represent sequential stimulus positions over the 2-s period, and the continuous black line is the high-resolution raw position trace including blinks and saccades. S05 generally has poorer tracking performance among participants. (c). Three example traces for participant S30 in the same format as b. This shows from left to right: 16°/s and 4°/s antigravity cases, and then a 4°/s gravity case. S30 typically shows better performance for the task. Each example is illustrated inside a reference square of sides 1,000 by 1,000 pixels with 100 pixel reference gradations along the vertical and halfway gradations (500 pixel) along the horizontal. Note that the five are example cases from over 14,000 trials recorded

From its spatial and temporal tuning properties, smooth pursuit has been suggested to have an underlying sensory processing substrate in which extra-striate human cortical motion area MT plays a key role (Debono, Schutz, Spering, & Gegenfurtner, 2010). The fast, fine control of motion direction estimation requires the use of inhibitory and excitatory neural computations within spatiotemporal channels encoding direction in a balance with a dynamic evolution over tens of milliseconds (Medathati, Rankin, Meso, Kornprobst, & Masson, 2017; Pack & Born, 2001; Xiao & Huang, 2015). Disrupted balances in synaptic level neural interactions have been linked to atypical sensorimotor processing in models of both autism spectrum disorder (Lee, Lee, & Kim, 2017) and schizophrenia (Murray et al., 2014). For schizophrenia, deficiencies in smooth pursuit and antisaccade performance attributable to poor inhibition have been identified as a phenotype of clinically diagnosed patients and their first-degree relatives (Myles, Rossell, Phillipou, Thomas, & Gurvich, 2017). One hypothesis for atypical smooth pursuit and other symptomatic sensory behaviours is that efferent neural signals called corollary discharge generated by the brain (separately in parallel to sensorimotor networks) to indicate self-actions like eye movements made within a dynamic environment contribute to online predictive computations (Bogadhi, Montagnini, & Masson, 2013; Orban de Xivry, Coppe, Blohm, & Lefevre, 2013). This predictive process can be impaired by deficits in inhibition with neurocognitive consequences (Crapse & Sommer, 2008; Fletcher & Frith, 2009). Thus, visual tracking tasks with continuous measures of performance dynamics provide a test case for contrasting hypotheses about hierarchical mechanisms behind deficits in schizophrenia and other neuropsychiatric disorders (Adams, Perrinet, & Friston, 2012; Faiola, Meyhöfer, & Ettinger, 2020). Schizophrenia is a heterogeneous disorder, and related traits within a healthy population captured by schizotypy also have a diverse set of associated behaviours which have been categorised by some as positive, negative or disorganised (Raine, 1991). In addition, some of the traits and behaviours associated with schizotypy are also found to overlap with behaviours associated with depression and anxiety (Lewandowski et al., 2006). Whether prediction deficits can be specifically associated with schizotypy is an outstanding question.

Our paradigm offers a novel window into individuals' sensorimotor processing. Predictive mechanisms in visual tracking have previously been measured in tasks involving blanking or occlusion of tracked objects (Bogadhi et al., 2013; Land & McLeod, 2000), analysis of tracking around a ball bounce (Diaz, Cooper, Rothkopf, & Hayhoe, 2013; Mann, Nakamoto, Logt, Sikkink, & Brenner, 2019) and prediction of whether a ball will hit a future target or be intercepted (Brenner, Smeets, & de Lussanet, 1998; Spering, Dias, Sanchez, Schutz, & Javitt, 2013) among other related previous experiments, too numerous to include. These tasks elucidated the key role of extrapolation processes in estimating future locations and suggest a critical role for prediction along the trajectory (Bansal, Ford, & Spering, 2018). Three outstanding questions formed the bases for the hypotheses tested in the present work: (a) Can participants accurately track a naturalistically accelerating moving ball within a background with impoverished target depth and size cues? (b) Will the inversion of gravity have a measurable effect on tracking? (c) Is there evidence that schizophrenia-associated trait levels have any link with individual performance and does this depend on the gravity conditions? To obtain answers, we ran the experiments collecting a large multivariate set of data with the novel task. In addition to testing the hypotheses related to questions (a) to (c) for our inferential statistics, we sought to obtain useful visualisations and accompanying descriptive statistics particularly around performance dynamics to aid in the conceptual understanding of this untested configuration. These could be important for scientific posterity, in the light of the multidisciplinary nature of the questions of interest, to ensure the work provides useful insights to behavioural, computational and clinical researchers by illuminating potential follow-up questions.

2 | METHODS

2.1 | Participants

We tested 44 individuals (28 females, Age $M = 26.4$, $SD = 9.2$) including students and staff recruited by opportunity sampling at Bournemouth University. Each participant received £5 for their participation. The study was approved by the Research Ethics Committee of Bournemouth University and carried out in accordance with the principles of the Declaration of Helsinki. The number of participants could not be determined by a standard power calculation as the experiment combined existing tools in a novel configuration. To pre-determine the target number of participants, we therefore considered the statistical power within the eye-tracking tasks and the trait measures separately. First, from previous tasks in which differences between conditions of motion direction or spatial orientation were compared using dynamic eye-tracking measures including saccades and tracking performance, medium effect sizes were obtained with 7 to 9 participants in within-participants designs (Meso, Montagnini, Bell, & Masson, 2016; Meso, Rankin, Faugeras, Kornprobst, & Masson, 2016). Second, in a previous task in which the schizotypy inventory (the SPQ) was used to quantify traits in a study of the link between scene scanning patterns and schizotypy, small effect sizes of $r < 0.3$ were obtained for one of the hypotheses using just 30 participants in a correlational design (Hills, Eaton, & Pake, 2016). The second of these experiment components involving the trait measures was therefore the part that critically determined the participant numbers. With SPQ as our primary trait measure

of interest, we took the minimum numbers of $N = 30$ for a small effect size from the Hills et al. study as our starting point and added 50% to obtain a target of $N = 45$. This target number was high enough not to limit the power of the control General Health Questionnaire, which has been shown to have a high sensitivity to mental state (Hu, Stewart-Brown, Twigg, & Weich, 2007), and the Beck Anxiety Inventory which has been demonstrated to measure trait anxiety in validation samples as low as 40 (Fydrich, Dowdall, & Chambless, 1992). During data collection, participants were occasionally excluded for various reasons such as failure to meet normal visual acuity requirements, withdrawn consent before experiment completion and late arrival for experimental sessions. While in the data collection phase, the target N remained the same compensating for these exclusions. After data collection was completed, during inspection and validation of eye traces, two participants were found to have particularly noisy eye position data, possibly because of poor pupil tracking. Data for one of these participants had to be excluded because the high-frequency noise was much larger than the precision of the tracker. For the second participant, data were usable after the exclusion of about15 trials. Valid data were therefore eventually collected for 44 participants after application of the described exclusion criteria.

2.2 | Materials (Stimuli)

Stimuli were generated on a Windows 7 PC running bespoke MATLAB (MathWorks) routines supported by the Psychtoolbox video control libraries (Brainard, 1997; Pelli, 1997). Visual stimuli were presented on a 21' BenQ LED Source Eye 120 Monitor with a resolution of 1,920 × 1,080 pixels and 100 Hz refresh rate. The monitor was placed 80 cm from participants, and eye movements were recorded from the right eye using an SR EyeLink video eye tracker operating at 1,000 Hz. During tracking, participants' movements were restricted by a head- and chinrest.

On each trial, the stimulus was displayed in the central region of a full-screen mid-grey (15 cd/m^2) background within a virtual square with invisible/unmarked sides of 900 pixels or 19.3 degrees of visual angle (°) (see Figure 1a). The task contained a black ball of size 0.34° diameter which moved with motion characterised by Equations (1) and (2) for the horizontal and Equations (3) and (4) for the vertical motion.

$$P_x(t) = \int_0^t V_x(t)\mathrm{d}t = X_o + S_x t \tag{1}$$

$$P_x(t) = \int_0^t V_x(t)\mathrm{d}t = X_o + S_x t \tag{2}$$

where V_x is the constant horizontal component of the speed with values of S_x set at ±4°/s or ±16°/s for the slow and fast conditions. The ball moved to the right (+) or left (−) in a randomised order, making the horizontal direction unpredictable in each trial. The time-varying horizontal position is given by P_x, a linear function of the initial speed S_x, with a constant starting point at the horizontal centre of the screen, X_o.

$$V_y(t) = S_y + gt \tag{3}$$

$$P_y(t) = \int_0^t V_y(t)\mathrm{d}t = Y_o + S_y t + (gt^2)/2 \tag{4}$$

V_y is the time-varying vertical speed component which is initiated as S_y with values randomly picked from a flat continuous distribution within the range of ± [2 to 2.5]°/s away from the direction of g. The acceleration due to gravity g is set to ±9.81°/s^2 for the gravity (+) and antigravity (−) conditions. For the stimulus circle of 0.34°, this generates on-screen motion expected for a ball 40% bigger than a full-sized basketball (which is 23.9 cm in diameter). There are no explicit pictorial clues beyond this acceleration to the absolute size or depth of the stimulus ball, making the task less rich in visual cues than previous interception and tracking tasks.

2.3 | Procedure

Participants were screened for normal or corrected-to-normal vision with a visual acuity letter chart. Bespoke MATLAB programs with a mouse to check selected Likert scale items on a screen were used for three inventories, the 12-Item General Health Questionnaire (GHQ) (Hardy, Shapiro, Haynes, & Rick, 1999), the 74-item Schizotypal Personality Questionnaire (SPQ) (Raine, 1991) and the 21-item Beck Anxiety Inventory (BAI) (Beck, Epstein, Brown, & Steer, 1988) presented before, in between and after the tracking experiment blocks, respectively. The tracking task was separated into two blocks of gravity and antigravity trials presented in a counterbalanced order across participants. Each block had 160 trials, each 2 s in duration with a participant button press to initiate stimulus onset after a 1-s interstimulus interval. Each trial started with a 500 ms central circular dark grey fixation spot on the mid-grey screen which disappeared at trial onset. The stimulus was followed by a grey screen (see Figure 1a for task sequence). Participants were instructed to fixate whenever the central spot was present and track the moving ball on the screen as well as they could until it disappeared, and this was achieved to different degrees by participants (see, e.g., Figure 1b-c). Each block contained 80 fast and 80 slow trials and lasted approximately 12 min so that after

a few trials at the start, the direction of gravity was quickly predictable within each block. The full experiment took about 30 min per participant.

2.4 | Design

We used a multivariate within-participants design. The independent variables were Gravity direction with two levels, Gravity (G) and Antigravity (AG), and Horizontal Speed with two levels, Slow (S, 4°/s) and Fast (F, 16°/s). The five dependent variables were SPQ, GHQ, BAI, RMSE (with fifty performance values organised as 2×25, that is the two representing the orthogonal directions x or y; and 25 values as averages every 20 ms from onset—20 ms, 40 ms, 60 ms, ..., in the range 0–500 ms) and Saccades (x2, rates and sizes). We also recorded participant AGE and SEX as demographic variables during the experiments. Our three questions of interest (a) to (c) generated four hypotheses. H1: If participants are particularly good at tracking under gravity, then performance dynamics for constant speed x-RMSE and accelerating y-RMSE will be the same; and this may depend on gravity direction. H2: If antigravity substantially disrupts tracking, then there will be an effect of gravity direction on the vertical y-RMSE dynamics revealing the time course of antigravity processing. H3: If a prediction deficit measurably impacts antigravity tracking (more so than predictable gravity tracking), then SPQ traits will be specifically related to tracking metrics, RMSE and Saccades, in a way that depends on or interacts with gravity direction and is *not* explained by GHQ and BAI. H4: If the evidence supports H2 and H3, then through PCA, the multivariate data may enable us to characterise the relationship between the DVs and identify independent contributions to the variability including those specifically associated with schizotypy traits, prediction deficits and tracking.

2.5 | Data analysis

We identified and removed blinks and other instances of lost eye movement signals from the data using standard approaches previously described (Meso, Montagnini, et al., 2016; Meso, Rankin, et al., 2016). We extracted each saccade during the task and estimated the amplitude according to the algorithm of Engbert and Kliegl (2003), adapted for more sensitivity by reducing the median speed in the threshold parameter λ from 6 to 5 and enforcing a longer restriction between saccade events of 30 ms (Meso, Montagnini, et al., 2016). We filtered each individual trace with a 5th-order Butterworth filter with a cut-off at 50 Hz to remove the higher frequency noise components and identified the valid trials (which did not have intrusive blinks, large stimulus-independent movements or noise), excluding the few invalid ones, <2%, from the analysis. We computed the dynamic root-mean-square errors (RMSE) by calculating the absolute difference between the separate *x*- and *y*-axis stimulus positions (at 100 Hz, i.e. P_y and P_x of Equations 2 and 4) and the eye movement samples (averaged over every 10 ms to match resolution between eye tracker and screen) over time for each trial. This choice of RMSE as a variable makes the current work notably different to previous experiments on pursuit which focus on tracking gain as a key measure (Jorges & Lopez-Moliner, 2019; Spering & Montagnini, 2011). In our case, we made this decision to have a simple dynamic performance measure with no assumptions about directionality of errors or about the interaction of saccades and pursuit systems. This simplified metric may no doubt need to be decomposed into its parts in subsequent work. The result was a pair of horizontal and vertical values of RMSE in degrees (°) further averaged every 20 ms, matching the 50 Hz filtered resolution. This was then analysed from stimulus onset at 0 ms up to 500 ms. In order to provide a general feel for the dynamic performance in the tasks, we visualised the data in figures (e.g. Figure 2) using standard errors across participants for data separated by time bins plotted as shading around line traces to indicate the overlap, or otherwise, of compared pairs of dynamic traces. As a direct follow-up to these visualisations, for statistical inference, we compared conditions using two-tailed *t* tests of two types: repeated measures for the hypotheses contrasting the gravity direction conditions (H1 and H2) and independent samples for the comparison of the trait-level groups (H3). Over each of the 25 sample points along the section of the dynamic RMSE traces of interest (within the range 0–500 ms, i.e. 20 ms, 40 ms, 60 ms...), an alpha value of $p = .05$ was Bonferroni-adjusted to $p = .002$ before significance testing. Previous work on visual motion processing serving tracking has shown that there are essentially two phases of responses, an early closed-loop phase which is served by stimulus-driven bottom-up computations and a later open-loop phase gradually initiated from 150 to 200 ms involving recurrent top-down contributions for both volitional and reflexive tracking (Masson & Perrinet, 2012; Spering & Montagnini, 2011). In the current work, we were particularly interested in the point of transition from closed to open loop to allow us to contrast conditions in a way that might separate fast automated pre-attentive processes, of which acceleration due to gravity might be as it exploits a strong prior (Jorges & Lopez-Moliner, 2017), from potentially slower recurrent processing of acceleration as arbitrarily curved trajectories (Bennett & Benguigui, 2013; Bennett et al., 2007; Ross et al., 2017). To this end, we set 200 ms as a critical time point for our data analysis further comparing gravity and antigravity conditions. Visualising the tracking under the range of conditions in Figure 2 supports the notion that there was a critical performance time window between

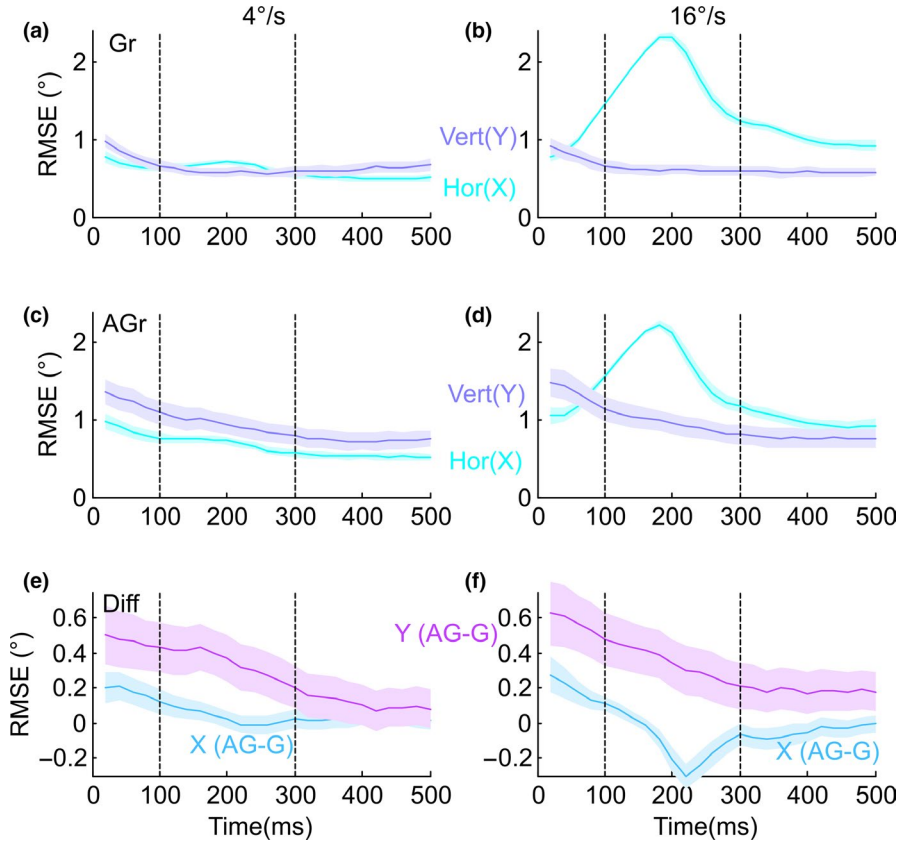

FIGURE 2 Gravity versus Antigravity dynamic root-mean-square error (RMSE) traces. (a) Position RMSE trace on the ordinate axis is plotted against stimulus time from onset (0 ms) on the abscissa for 44 participants averaged for the vertical (purple) and horizontal (cyan) values sampled every 20 ms over 500 ms. Shaded areas are standard error of the mean. This trace is the slow-speed gravity condition showing small standard errors with consistent performance across participants for both x- and y-RMSE. After onset, performance improves down to 0.5° in 100 ms. (b) This condition is the fast-speed gravity condition, and the trace colour codes are the same as a. Performance quickly improves for the purple trace with the same time course of 100 ms, but takes longer to do so for the cyan trace following a catch-up saccade required at the higher speed. (c) RMSE traces for the slow antigravity condition with similar colour coding to a. There is worse performance for up to 200 ms in the horizontal direction (cyan), and up to 400 ms in the vertical (purple) negative gravity-influenced direction. (d) RMSE traces for the fast antigravity condition with the same colour coding as c. The vertical performance difference (in magenta) shows the same trend as c, while the horizontal difference (blue) reduces to zero quicker than in c. (e) Two additional traces computing the difference between the gravity and antigravity RMSE traces for the vertical (magenta) and the horizontal (blue) components marked at the slower speed. (f). A similar trace to (e), for the faster speed condition also showing a delayed difference in the *y*-direction. Note that the horizontal axis is at −0.3 and not zero [Colour figure can be viewed at wileyonlinelibrary.com]

100 and 300 ms within which performance reached its peak so that pronounced differences in dynamics could be seen.

2.5.1 | Linear mixed-effects modelling

We directly tested H2 using a linear mixed-effects model to ask whether the RMSE performance at this critical value of 200 ms from onset was specifically dependent on the Gravity Direction (i.e. Gravity or Antigravity). As fixed effects, we used Gravity direction and Speed (without an interaction term), and as random effects, we had by-participant random slopes for the effect of Gravity Direction. In the syntax used in R, the formula for this model was "RMSE200 ~ 1 + GravityDir + Speed + (GravityDir|Subject)." A P-value was obtained using a likelihood ratio test of the full model (with fixed terms Gravity direction and Speed) against a NULL model constructed by removing the Gravity Direction (GravityDir) predictor. The model comparison produced a chi-squared value exploiting Wilk's theorem to compute the estimate from −2 × log-likelihood ratio as detailed in the chapter on hypothesis testing in the textbook by Casella and Berger (2002). We chose the likelihood ratio approach rather than reporting several fixed and random effects in our novel multivariate experiment to restrict our statistical inference specifically to the hypotheses we wanted to test.

For H3, we asked whether the saccade rates and/or the saccade amplitudes were specifically predicted by levels of SPQ rather than BAI or GHQ trait levels. Direct relationships between both saccade metrics and SPQ traits were quantified

using linear mixed-effects models. As fixed effects, we used SPQ, Gravity Direction and Speed. We included an interaction term between SPQ and Gravity to test the trait prediction hypothesis which we were specifically interested in. As random effects, we used intercept-only models for BAI and GHQ, and by-participant random slopes for the effect of gravity. Again, we compared the tested models to alternative null models and produced corresponding chi-squared values for significance testing. The formula of the tested models using R-syntax was "SacAmp ~ 1 + SPQ * GravityDir + S peed + (GravityDir|Subject) + (1|BAI) + (1|GHQ)" for the amplitudes and "SacRate ~ 1 + SPQ * GravityDir + Speed + (GravityDir|Subject) + (1|BAI) + (1|GHQ)" for the rates. In both cases, the corresponding null models were the same as above but without the SPQ term, retaining the GravityDir term. In the control models testing for BAI and GHQ dependence, respectively, in the R formulae above, there was a substitution of positions between the SPQ and BAI, or GHQ, terms. To run the linear mixed-effects models, we used the lme4 library in R (Bates, Mächler, Bolker, & Walker, 2015; R-Core-Team, 2019). Before all analyses, we visually inspected residual plots for deviations from homoscedasticity or normality.

2.5.2 | Pattern analysis and abstract feature extraction

To unpack some of the less obvious patterns within selected multivariate metrics of the rich data set, we used principal component analysis (PCA) to identify the dominant parametric relationships between our measures. PCA is among the oldest and most widespread multivariate techniques that reduce the dimensionality of a data set with interrelated original variables (m), transforming the meaningful variation to a new set of much fewer variables or principal components (r; such that the number of elements $n_m > n_r$), which are ordered from strongest to weakest and uncorrelated (Hotelling, 1933; Pearson, 1901). In other words, each component will combine contributions from multiple variables within m to capture an aspect of the data that is orthogonal to the rest of the data and therefore qualitatively different in how it should be interpreted. As such, it is useful as a means of providing insights about data obtained in a range of different fields, for example economics, biology, engineering or psychology, particularly when one has an understanding of what is measured by individual variables, but a bigger picture about how they come together remains elusive (Jolliffe & Cadima, 2016; Wegner-Clemens, Rennig, Magnotti, & Beauchamp, 2019). In the present case, we set $n_m = 32$, restricting our matrix to just a selective explorative subset of what might have been possible in an unconstrained data-driven approach. The data matrix included as dependent variable columns with information about AGE, SPQ, BAI, GHQ, five values of RMSE intended to capture the temporal evolution of tracking performance at five time points [100, 200, 300, 400 and 500] ms, and two saccade properties of Amplitude/Size and Rate. The seven ocular metrics, five RMSE and two from saccades were each obtained for four conditions across speed and gravity levels. The data produced a 44-by-32 matrix and the subsequent analysis reduced these to a limited set of n_r components from the PCA. Running PCA uses iterative fits of the data matrix to produce λ, a set of n_m eigenvalues of descending magnitude corresponding to the relative strength of the variance of each subsequent independent component. Each λ_i is the sum of contributions from the n_m elements of a corresponding eigenvector α, with one element for every variable of m providing a loading or weight quantifying how much it contributes to the PC_i with relative variance λ_i. Transformation between data space and PCA space can be done using matrix operations of λ with α. The analysis is implemented with MathWorks MATLAB and the Statistics toolbox using the eigenvalue decomposition method for the covariance matrix to estimate λ with α and the number of PCs n_r is determined by parallel analysis with a run of 1,000 iterations (Jolliffe, 2002; Ledesma & Valero-Mora, 2007).

The traits estimated by our three inventories SPQ, BAI and GHQ are known to have some comorbidity with each other. SPQ as a measure captures the heterogeneous symptomology of schizophrenia which includes positive, negative and disorganised symptoms (Raine, 1991). A subset of neural mechanisms which are implicated in schizophrenia are also found in models of depression (Samsom & Wong, 2015) and across all three of these inventories, there is 50+% comorbidity between diagnosed schizophrenia and depression, depression and anxiety and, to a lesser degree, schizophrenia and anxiety (Lewandowski et al., 2006). For these reasons, we expected some strong correlation identified during the analysis including these three inventories and these relationships will capture the common aspects of the traits. In such cases, it is expected that the comorbidities might explain a dominant proportion of the variance and as such take up one or more of the strongest principal components identified. The analysis would then have to consider more components than these initial ones which still remain above the threshold of noise; in this case, up to a number n_r is determined by the parallel analysis to take into account the less obvious structure of interest to us relating the trait and oculometric data beyond comorbidities (Jolliffe, 2002; Ledesma & Valero-Mora, 2007). What PCA allows us to do further is to separate these composite heterogeneous traits into potentially meaningful features in a data-driven way by identifying statistically independent relationships. For example, if evidence found while testing H3 supports a prediction hypothesis linked specifically to the SPQ and not the control inventories, then one might expect that SPQ will contribute to multiple independent PCA

components, but only one of these will be most strongly specifically related to prediction effects in tracking performance.

3 | RESULTS

3.1 | Tracking performance dynamics under Gravity and Antigravity

We first calculated the position RMSE which gave the dynamic absolute difference between where the stimulus appeared on the screen and where the eye was recorded to be in the same instant, thus serving as a simple performance measure. This was compared in separate plots for the slow and fast conditions both for the gravity and antigravity cases. The results shown in Figure 2 give the horizontal (x) and the vertical (y) RMSE components in the cyan and purple, respectively. For the slow gravity condition where the stimulus x- and y-speeds are more comparable than the faster speed (i.e. both in range 0.4–4°/s so within an order of magnitude), there is little difference between the horizontal and vertical RMSE traces (see Figure 2a, purple versus cyan) with both reducing to a minimum by 100 ms and standard errors fully overlapping suggesting, under H1, that there is no measurable difference between horizontal and vertical tracking under this condition. To isolate the effect of switching acceleration from gravity to antigravity, the differences between these conditions are plotted in Figure 2e-f. We find that the antigravity condition (Figure 2c-d) consistently resulted in worse performance than the gravity condition (difference traces in magenta and blue, Figure 2e-f). For the horizontal, this difference between antigravity and gravity performance decreases gradually before a plateau of about 200 ms from onset (blue trace, Figure 2e-f). For the vertical, the difference was more sustained and gradual in its reduction taking up to 400 ms or more to reduce to zero (magenta, Figure 2e-f). The fast condition had a large initial horizontal RMSE as participants typically initiated a larger catch-up saccade following onset latency (Figure 2b and d, cyan trace with a peak around 200 ms). The unfamiliar configuration of the antigravity condition degraded participant performance, despite many practice trials within the block. The standard errors in the shaded areas were larger under the antigravity conditions, showing that individual differences in performance increased more than twofold under that configuration. The respective standard deviations at 200 ms for the gravity and antigravity conditions at 4°/s are $G_X = 0.16°$ and $AG_X = 0.24°$ for the x-direction and $G_Y = 0.27°$ and $AG_Y = 0.65°$ for the y-direction. Using a 2-sample F test for equal variance on the gravity and antigravity traces: for x-directions, we find the variances to be significantly different from each other, $F\,(43) = 0.46$, $p = .012$, and for the y-direction, the difference is even more pronounced, $F\,(43) = 0.18$, $p < .001$. To test H2, linear mixed-effects analysis was used to estimate the prediction of the y-RMSE at 200 ms (within the critical time shown in Figure 2) with Gravity direction and speed as fixed effects and participants as random effects. There was a significant effect of gravity direction on vertical RMSE ($\chi^2(1) = 10.92$, $p = .00095$ and giving a large effect size of $d = 1.17$), increasing the tracking error by 0.36° $SE = 0.10°$ between Gravity and antigravity conditions at 200 ms.

3.2 | The link between trait levels and behavioural measures

The dynamic RMSE results in Figure 2 gave little specific indication of the individual differences beyond the standard errors for the antigravity condition, particularly for the vertical RMSE. To probe this further, we looked at the vertical traces only and asked whether the predictive element of the task manipulated across gravity conditions might interact with individual trait levels. To this end, based on their scores using the self-report SPQ inventory we split the 44 participants into a lower (range 2–15, $M = 10.1$, $SD = 3.8$) and higher (range 15–58, $M = 30.1$, $SD = 12.8$) schizotypy trait groups of equal numbers of individuals (Raine, 1991) to support the visualisation of any differences here. We found that there was complete overlap between the low and high SPQ individuals' performance traces under the gravity conditions (Figure 3a-b), with both groups performing very well. In the antigravity condition however, low-trait individuals (Figure 3e-f, black trace) had better performance than high-trait individuals for the first 400 ms with a less steep dynamic improvement of performance, that is less reduction of error over time and a better peak performance with an RMSE of 0.5° compared to about 1° after 400 ms. There was no significant difference between the dynamic performance of the groups in the gravity condition but in the antigravity condition, between 300 and 500 ms at least four samples representing 80 ms of comparison between the high- and low-trait groups were significantly different ($p < .002$) from each other in both speed conditions in Figure 3e and 3f, seen in the separation of the black and red curves after the dashed line. This tracking generated on average 2–5 saccades per second, and from these, we quantified the averaged rates and sizes, looking at how these metrics related to individuals' SPQ scores. We tested these using linear mixed-effects analysis to predict the saccade metrics (rates and size) from fixed factors of SPQ, Gravity direction and Speed, and participants, BAI and GHQ were used as random effects in an analysis detailed in section 2.5.1. The NULL model was identical but with the SPQ fixed factor omitted. For the gravity condition, there was a slight trend towards lower rates for participants with higher SPQ scores but no significant relationship with saccade rates (Figure 3c). There was no evidence in comparison with the NULL model that

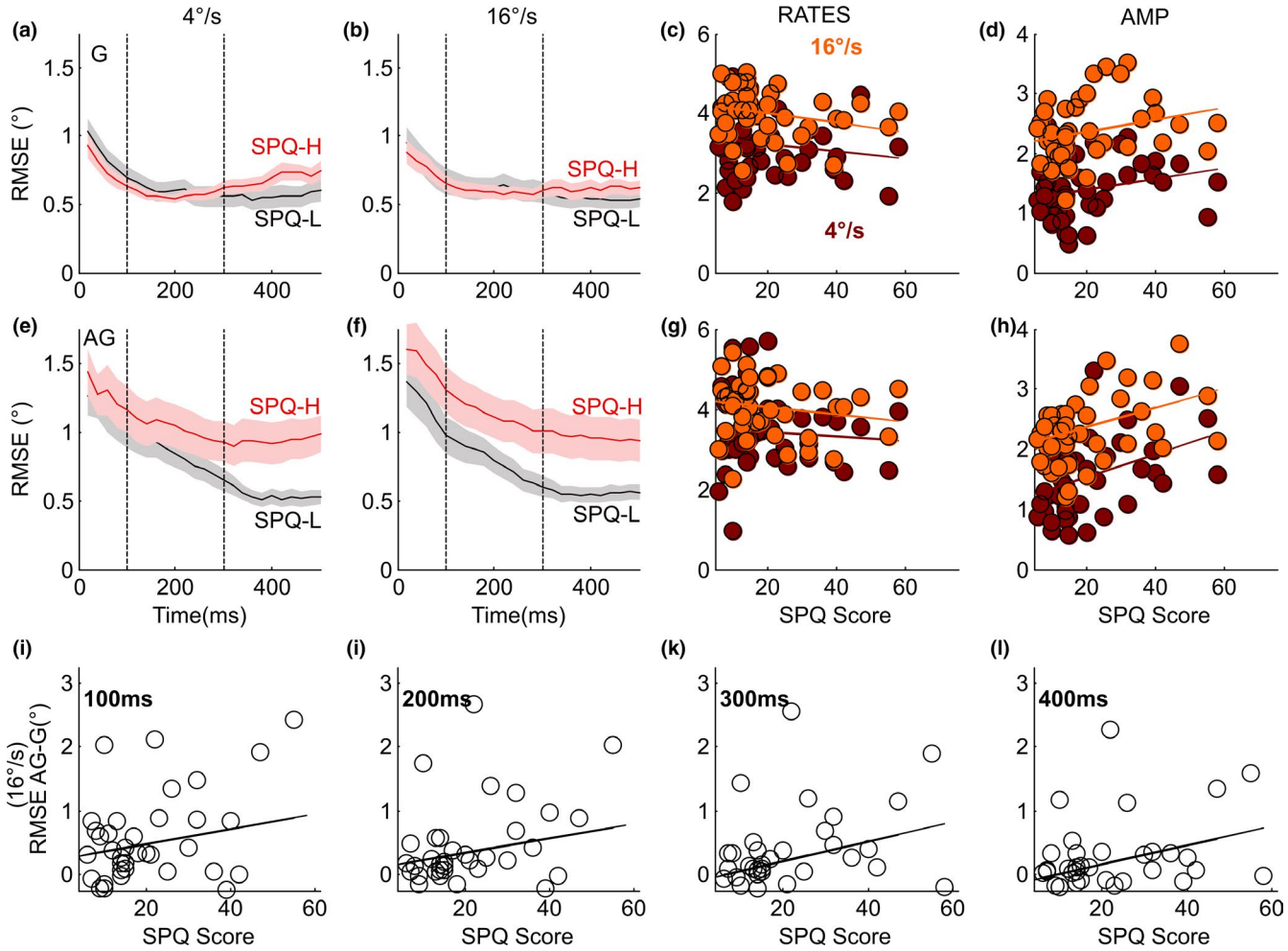

FIGURE 3 RMSE and Saccade performance for gravity (top row) and antigravity (bottom row) conditions separated by SPQ trait levels. (a) The vertical component of the RMSE on the ordinate axis is plotted against stimulus time from onset on the abscissa. Two averaged traces are shown, comparing participants equally separated into a low SPQ trait group (black) and a high SPQ group (red). Performance traces cannot be separated up to 400 ms. (b) RMSE traces with similar colour coding to a show no differences between the low and high SPQ traces for the fast case. (c) The saccade rates in the ordinate axis are plotted against the SPQ score in the abscissa showing averages for all individuals during the fast (orange) and the slow (maroon) stimuli presentations with a difference of about 1 saccade/s between them. There is a negative trend for each indicated by the linear fit. (d) The saccade amplitudes/sizes are plotted against the SPQ score for each participant with slow (maroon) having a very similar trend to the fast (orange) linear fits, both increasing with SPQ. (e) The vertical direction RMSE plot for the antigravity condition in the same format as a. The lower SPQ trait cases (black) show steeper and faster gradual improvement than the higher SPQ cases (red) with all antigravity cases showing more gradual, delayed improvement than under the gravity condition. The plateau of performance after 400 ms has a larger difference (0.5°) between low and high traits than the gravity condition. f. The trend is similar to the slow condition in e. (g) Antigravity condition saccade rates against SPQ score show the same results as c. (h) Saccade amplitude against SPQ score illustrates a positive relationship with SPQ for both fast and slow stimuli, a trend which appears to be stronger under the gravity condition in d. (i) For the faster speed condition, the relationship between individuals' SPQ scores (abscissa) is plotted in a scatter graph against the difference between the antigravity and gravity RMSE values (ordinate) first for 100 ms, as a visualisation of the interaction of gravity and trait. A least squares linear fitted trend line is included for visualisation. Similar plots are shown for subsequent time points, (j) 200 ms, (k) 300 ms and (l) 400 ms [Colour figure can be viewed at wileyonlinelibrary.com]

SPQ scores affected the saccade rate ($\chi^2(2) = 1.60$, $p = .449$). The rates were generally higher by almost one per second for the fast compared with the slow condition, implying more frequent catch-up saccades during the faster and therefore more difficult tracking task. The same analysis was done for the saccade amplitudes. There was a significant effect of SPQ on saccade amplitude ($\chi^2(2) = 8.96$, $p = .0113$, with a medium effect size estimated by Cramer's $V = 0.323$), indicating higher SPQ resulted in higher saccade amplitudes. The results generally suggest that individuals with higher SPQ scores tended to produce larger saccades than those with lower scores under both the gravity condition (Figure 3d) and the antigravity condition (Figure 3h), with it even more pronounced in the latter case. We plot SPQ against the difference

between RMSE for the antigravity and gravity conditions at four time points to visualise trait dependence (Figure 3i-l).

The SPQ captures behavioural traits specifically related to schizotypy. It is unclear whether the trends identified in RMSE dynamics and saccade amplitudes in Figure 3 are specific to the SPQ or more broadly reflective of mental function or state. To explore the broader relationship between other traits and the tracking task, we similarly plotted results from two further established trait inventories. The short General Health Questionnaire, GHQ (Hardy et al., 1999), was used to separate participants into two equal groups (low range −16 to −7, $M = -10.6$, $SD = 2.7$; and high range −7 to 10, $M = -2.3$ $SD = 5.1$) and look at how these related to the set of eye-tracking measures used in Figure 3. The BAI, an anxiety trait measure, was similarly used (low range 0 to 8, $M = 3.6$, $SD = 2.8$; and high range 8 to 46, $M = 18.0$ $SD = 10.5$). As there was little substantial difference between fast and slow conditions in Figure 3, for the visualisation we focused on the slow conditions at 4°/s. We first looked at the dynamic RMSE traces for the vertical direction comparing a low GHQ averaged group (black) corresponding to negative states with a high GHQ group (red) in Figure 4a and e. Under the gravity condition, there was a very small offset of 0.1° between the pair of traces, with lower trait individuals doing slightly worse but both notably reaching plateau performance within the first 150 ms. Under the antigravity condition however, the curves were surprisingly separated by about 0.4° so that the low GHQ cases (black traces) showed worse performance across the full duration considered up to 500 ms from onset than the high GHQ cases (red) and this was true for both the fast and the slow stimuli. This visible tendency towards a difference was not statistically significant in the dynamic comparison, with $p \gg .002$ for all compared pairs in the range 0–500 ms. We similarly used the BAI trait measures to separate RMSE traces. Under the gravity condition, the low anxiety trait group (black) were similar in performance for most of the range to the high anxiety trait (red) except for a small advantage, −0.2°, to the low-trait group around 200 ms (see Figure 4b). For the antigravity condition, there was a very small offset of ~0.2° across the range

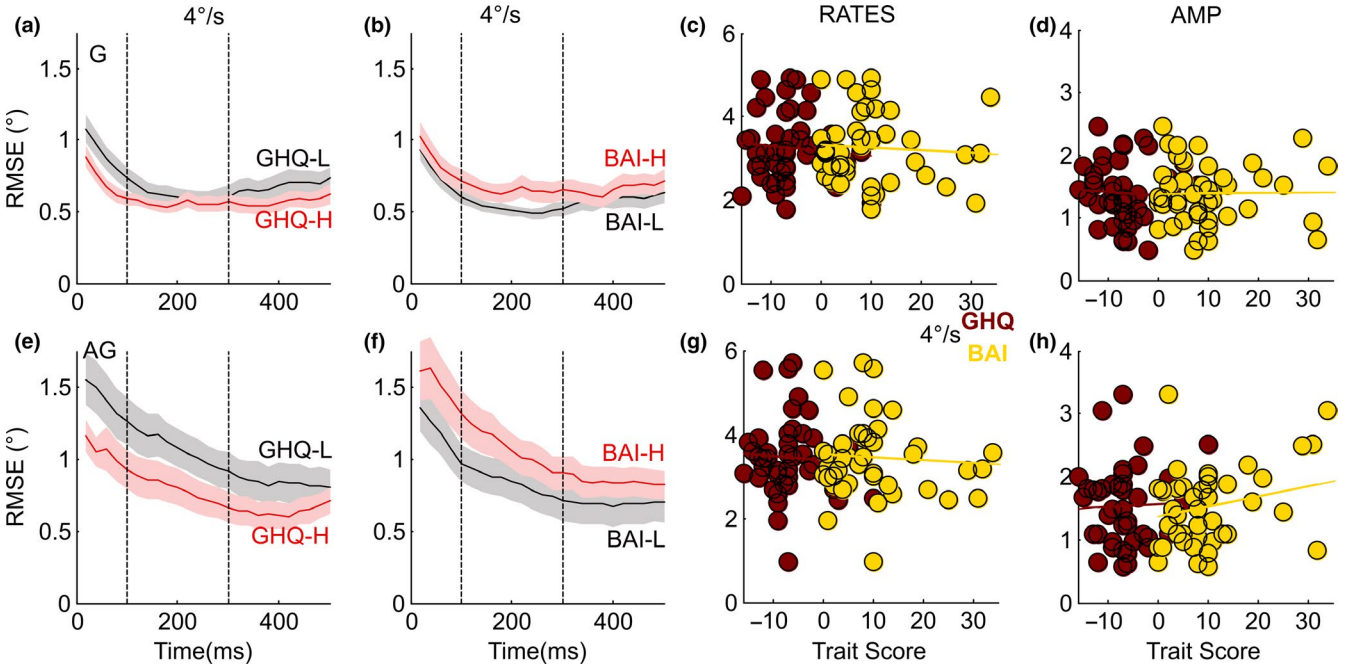

FIGURE 4 RMSE and Saccade performance at the speed of 4°/s for gravity (top row) compared to antigravity (bottom row) grouped by GHQ and BAI trait scores; see text for details. (a) The vertical component of the RMSE on the ordinate axis is plotted against stimulus time from onset on the abscissa. Two averaged traces are shown, comparing participants equally separated into a low GHQ trait group (black) and a high GHQ group (red trace). Performance is approximately equal across the range but slightly better for the low group by about 0.2°. (b) RMSE traces with similar colour coding to a, for the BAI. The low- and high-trait cases overlap except briefly around 200 ms. (c) The saccade rates on the ordinate axis are plotted against the trait scores (separately for GHQ in maroon circles and BAI in yellow circles) showing averages for all individuals during the slow stimulus trials. There is no significant trend in the linear fits. (d) The saccade amplitudes are plotted against the trait scores (GHQ and BAI as in c) for each participant again with no significant trend. (e) The vertical direction RMSE plot for the antigravity condition in the same format as a. The lower GHQ trait cases (black) show worse performance than the higher GHQ cases (red) by about 0.4° across the presentation duration under the gravity condition. The small difference is not found to be statistically significantly. (f) For the BAI, where high trait is negative, the trend is very similar to **E** with sustained worse performance for the high BAI cases (red) with a smaller difference of ~0.3°, again a difference which is not statistically significant. (g) Antigravity condition saccade rates against GHQ and BAI trait scores show no significant trend. (h) Saccade amplitude against GHQ and BAI trait scores shows no significant trends [Colour figure can be viewed at wileyonlinelibrary.com]

with low-trait individuals (black trace) performing better (see Figure 4f), though this difference was not statistically significant. Notably, a key difference between the SPQ and control GHQ and BAI RMSE traces can be seen by looking in between the marked vertical lines at 100 and 300 ms in Figures 3e-f and 4e-f, where the pair of SPQ groups shows a zero difference starting off from the same initial RMSE around 1.4°, whereas the controls (GHQ/BAI) start off with worse performance for the negative trait case. These dynamics imply overall poorer performance, including imprecise fixation for the control trait comparisons, while SPQ differences which become prominent under the antigravity condition are specific to initiation and eventually to maintenance of tracking. We similarly considered the saccade parameters and their relationship with GHQ/BAI scores. In two further linear mixed-effects analyses, we substituted the GHQ and the BAI for the SPQ by moving these controls from random effects to fixed effects in the analyses, and vice versa for the SPQ, and then testing this model against a NULL alternative in which the control fixed effect was omitted. In both cases, no significant effect of the two traits as predictors of saccade metrics ($p > .05$ in the χ^2 model comparisons), amplitude or rates, was measured, consistent with the trends plotted (Figure 4c-d and g-h). Within the earlier part of the dynamic RMSE plots, the SPQ traits seemed to capture a feature of the individual performances that the control groupings were insensitive to. The specific trends in the saccade amplitudes and the form of the RMSE curves might be associated with the known atypical inhibitory processing which occurs with schizophrenia and schizotypy.

3.3 | Principal component analysis for feature extraction

Finally, we used principal component analysis (PCA) to look at the main independent dimensions or features in our multivariate data set using a selection of our demographic and sensorimotor measures. We expected some relationships between our trait measures, and possibly age, due to the known comorbidity between the traits related to the pathological states the three inventories used attempt to capture. We sought to use the independent features identified by the analysis to separate out these heterogenous comorbidities and identify those related to the tracking performance, specifically those which might be associated with a prediction hypothesis. The set of 32 metrics included the four trait and demographic measures of AGE, SPQ, BAI and GHQ along with seven eye movement metrics including five dynamic y-RMSE metrics, saccade rates and saccade amplitudes, each repeated four times across the speed (S/F) and gravity (G/A) conditions (i.e. SG, SA, FG, FA). The aim was to allow us to

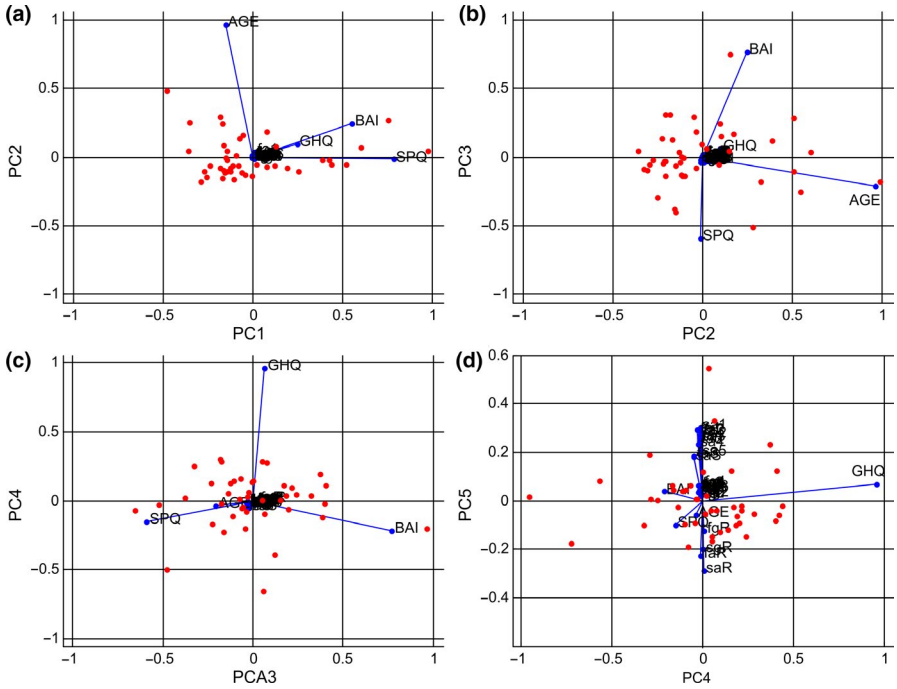

FIGURE 5 PCA results focusing on the first five components. (a) Projection of the data (small red circles) and the variable coefficients α (blue lines) onto the PCA space for the first two components. PC1 is dominated by SPQ with a contribution by BAI and to a lesser extent GHQ. PC2 includes AGE and small weights for BAI and GHQ but no SPQ. (b) Components PC2 plotted against PC3 in the same format as a. SPQ and AGE are weighted in an opposite direction from BAI, which dominates PC3. (c) PC3 versus PC4 shows PC4 to be strongly dominated by the GHQ. (d) PC4 versus PC5 shows the eye movements start to make a contribution to the components with the rate and size components aligned in opposite directions along the vertical axis (see α values in Table 1) [Colour figure can be viewed at wileyonlinelibrary.com]

cluster related measures from this selected subset and evaluate whether any identified abstract features could be used to infer specific processes and underlying mechanisms. Using a Bartlett test for dimensionality, we found that most of the measures contributed, that is $N = 26$, were needed to explain the variance of the input data with an alpha level of $p = .01$. This figure of variance from over 80% of the measures contributing suggests that the relationships which were identified with PCA reflected a heterogeneous set of underlying mechanisms which we sought to unpack. We used parallel analysis to estimate how many principal components were required to capture systematic variance from the contributing data variables (Ledesma & Valero-Mora, 2007). The resulting estimate was that this was achieved by the first five components, and the total variance collectively explained by these was 99.1%. In the current work, we focussed on these five PCs remaining aware that in future work with more data, additional components may also be found to be meaningful. We plotted the normalised projection of the variable (α) and data coefficients in pairs along the planes representing the five principal components (see Figure 5 and Table 1). This allowed us to consider each component in turn.

The first component, PC1, has the SPQ as the dominant variable contribution with BAI as second (both with weights over 0.5) and then GHQ. There are some inconsistent contributions from eye metrics particularly for antigravity, but

TABLE 1 The 32 measured variables from the experiment are listed grouped by measure type in the first column with each variable name included in the third column. The coefficients α which scale from −1 to 1 returned during the principal component analysis are shown to 2 dp with the highest three absolute values in bold. In the case of the fifth column where several coefficient values clustered around similar levels of 0.2–0.3, more than three values are highlighted with the higher half of the values all in bold

			PC Number and Coefficient				
Measure type	Metric #	Name	1	2	3	4	5
Demographic	1	Age	−0.15	**0.96**	**−0.21**	−0.04	−0.06
	2	SPQ	**0.78**	−0.02	**−0.59**	**−0.15**	**−0.10**
	3	BAI	**0.55**	**0.25**	**0.76**	**−0.22**	0.04
	4	GHQ	**0.24**	**0.10**	0.06	**0.96**	0.07
Slow G	5	100 ms	0.00	0.02	0.01	−0.02	0.03
	6	200 ms	0.00	0.01	0.01	0.00	0.03
RMSE	7	300 ms	0.00	0.01	0.01	0.00	0.05
	8	400 ms	0.00	0.01	0.01	−0.02	0.06
	9	500 ms	0.00	0.00	0.01	−0.03	0.06
Saccades	10	Amp	0.01	−0.01	−0.02	−0.02	0.05
	11	Rate	−0.01	0.00	0.02	0.00	**−0.20**
Slow A	12	100 ms	0.00	0.03	−0.03	−0.01	**0.30**
	13	200 ms	0.01	0.02	−0.03	−0.02	**0.27**
RMSE	14	300 ms	0.01	0.01	−0.03	−0.02	**0.26**
	15	400 ms	0.01	0.00	−0.03	−0.03	**0.23**
	16	500 ms	0.01	0.00	−0.03	−0.02	**0.19**
Saccades	17	Amp	0.01	0.01	−0.03	−0.05	**0.18**
	18	Rate	0.00	−0.01	0.01	0.00	**−0.29**
Fast G	19	100 ms	0.00	0.02	0.01	−0.03	0.03
	20	200 ms	0.00	0.01	0.01	−0.01	0.02
RMSE	21	300 ms	0.00	0.01	0.01	−0.01	0.05
	22	400 ms	0.00	0.01	0.00	0.00	0.07
	23	500 ms	0.00	0.01	0.00	−0.01	0.06
Saccades	24	Amp	0.01	−0.01	−0.04	−0.01	0.06
	25	Rate	−0.01	0.01	0.02	0.01	**−0.12**
Fast A	26	100 ms	0.01	0.04	−0.03	−0.03	**0.29**
	27	200 ms	0.01	0.01	−0.03	−0.01	**0.28**
RMSE	28	300 ms	0.01	0.00	−0.03	−0.01	**0.28**
	29	400 ms	0.01	0.00	−0.03	−0.02	**0.26**
	30	500 ms	0.01	0.00	−0.03	−0.02	**0.25**
Saccades	31	Amp	0.01	0.01	−0.04	−0.05	**0.18**
	32	Rate	−0.01	0.00	0.01	−0.01	**−0.23**

these have very small weights of <0.02 (Figures 5a and 6a and Table 1). We believe that this component captures a non-specific largely age-independent comorbidity between the traits, for example similar to that suggested by Lewandowski et al. (2006), capturing the variation of *negative mood levels* which are not strongly associated with age. PC2 is overwhelmingly dominated by AGE (Figure 5a and b) and notably has an almost zero weight for SPQ. BAI and GHQ have small weights here, and the early part of the y-RMSE (100–200 ms) also has very small weights of <0.03. This component may capture *age-related differences in mental state*, perhaps also mildly associated with anxiety differences across the lifespan. These first two components dominated by the traits and AGE account for 85.3% of the variance.

The third component, PC3, is dominated by BAI, with a weight of over 0.75, and has a negative relationship with SPQ (weight −0.6) and AGE (weight <|0.25|). This is the first component that gives us a small but consistent difference in weights between the eye metrics (excluding saccade rates) in the gravity and antigravity conditions (see Figure 6c and Table 1). The antigravity conditions have weights of −0.03 to −0.05, with little change across the dynamics, while the weights in the gravity condition are positive. This component captures associations between anxiety traits and a subset of schizotypy traits, with the higher anxiety trait scores associated with low levels of the corresponding SPQ dimension. This *anxiety-SPQ* feature likely isolates and reflects the generally sustained poorer tracking performance under the antigravity condition seen for the high BAI trait group in Figure 4f. The fourth component, PC4, is overwhelmingly dominated by GHQ with a weight of over 0.95. The next closest weight is BAI with a negative weight <|0.25|. PC4 may capture the *positive mood* aspect of the GHQ trait questionnaire as the strong weight for GHQ comes with a negative relation to the other trait measures within this component. There

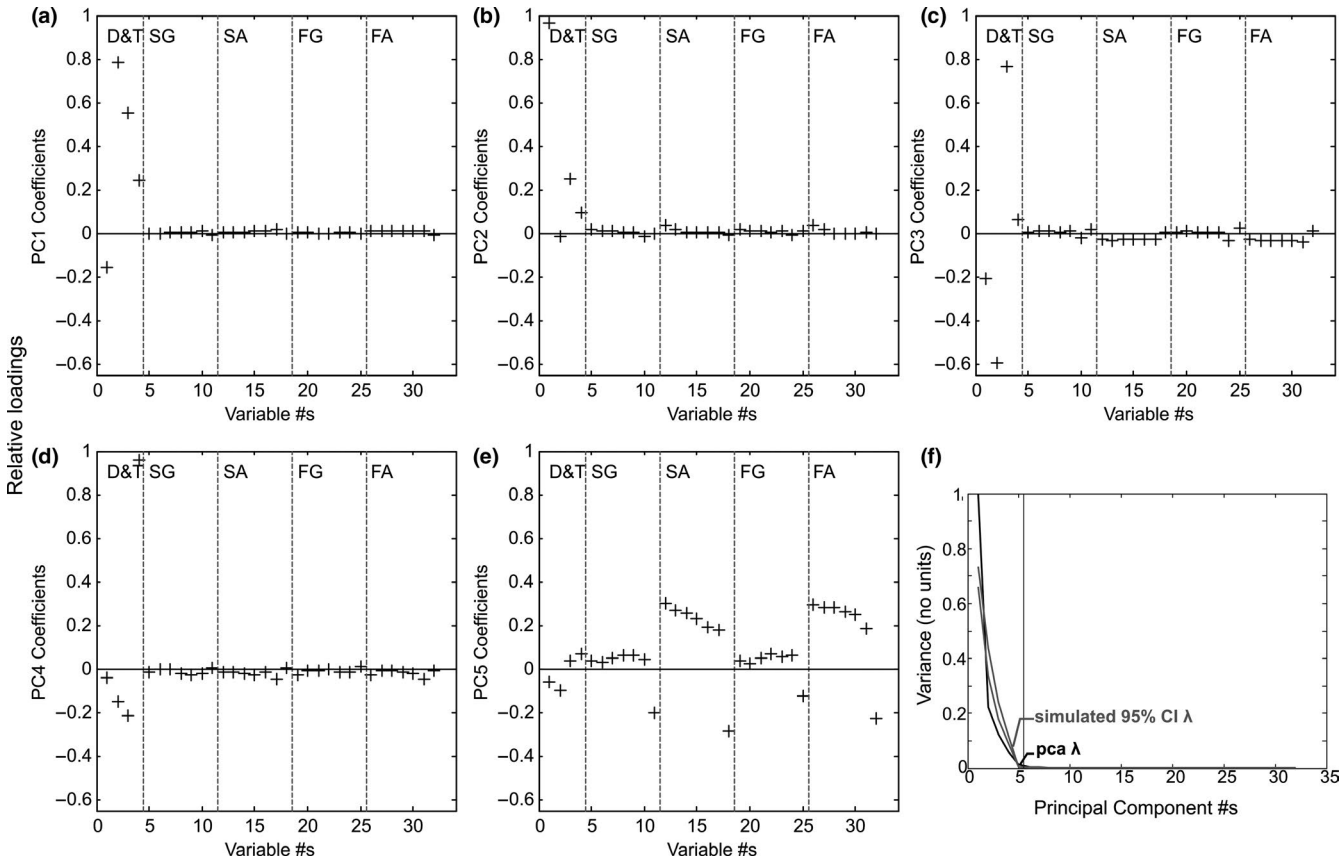

FIGURE 6 The relative loadings/weights α of each of the variables in PCA space. The numbered variables are detailed in Table 1. (a) For PC1: A plot of the relationship between the normalised weights once projected onto PCA space for each variable, compared for the first PCA component. Only the traits/demographics in the first column (#1-4) contribute. (b) PC2: Only the demographics/traits (# 1–4) contribute. (c) PC3 is dominated by variables #1-4, in particular #3, BAI, and there is some relationship with eye movement measures under antigravity. (d) PC4 is dominated by #4, GHQ. (e) PC5 is dominated by the eye-tracking measures, particularly under the antigravity conditions (#12–18 and #26–32) with maximum values around 0.27–0.30, lower than 0.76–0.96 for PC1-4. The strongest trait weighting is for SPQ at −0.10, about one third of the maximum value, and there is a temporal component such that variability at 100 ms is more important that that at 500 ms for the y-RMSE measure. (f) Results of the parallel analysis showing the variance eigenvalue λ (in black) plotted for each component (along the abscissa) and simulated bounds of the meaningful variance (grey). The vertical line shows the cut-off point just after PC5, where variance is estimated to become unsystematic

are no specific patterns in the related eye metrics with weights under 0.04. Overall, the first four components seem to capture variance dominated by AGE and the three inventories, with little contribution from the eye metrics. Within the first four PCs, we established what appeared to be features capturing (a) *negative mood*-related comorbidity, (b) *age*-related effects, (c) an *anxiety-/schizotypy*-associated dimension and (d) a *positive mood* factor. The Bartlett test identified 26 variables with systematic variation so we expect that the remaining 22 should contribute more to subsequent components.

PC5 is dominated by the dynamic vertical RMSE values, and in particular, those under the antigravity condition. Three striking patterns within this data are notable for us: (a) the difference between gravity and antigravity performance weights, specifically within the five y-RMSE values and the saccade size. While saccade rates also have a strong weight, this does not depend on gravity direction strongly (see Figure 6e). This tells us that PC5 reflects an underlying mechanism which drives variability in individual performance, most specifically under the antigravity stimulation. (b) There is a dynamic change in the weights under the antigravity condition, and this seems to capture what is visualised in the dynamic y-RMSE traces of Figure 3a/b when compared to Figure 3e/f. Initiating the first 100 ms of the eye movement under the antigravity condition has the most variability across participants, and this systematically reduces at 200 ms and subsequently with every other PC5 weight until 500 ms. This dynamic aspect captures the strangeness of the antigravity condition (in contrast to the expected gravity condition where the variance is larger at 300–500 ms than 100–200 ms) experienced at the onset of every stimulus trial. The reduction in the weight over the course of 500 ms is consistent with the implementation of a compensation mechanism which eventually brings performance back into line. We believe these dynamics make PC5 a candidate for a dynamic prediction mechanism. (c) The strongest of the trait/demographic weights is SPQ at just over −0.10 or one third of the maximum coefficients of the RMSE values of approximately 0.3 (see Table 1). With most of the variance related to the SPQ in the data strongly associated with the other trait/demographic measures explained by PC1 and PC3, what remains in the weight of the SPQ in PC5 captures variance associated with a mechanism specific to antigravity (c.f. (1)) and which has a dynamic processing element to it (c.f. (2)). This relationship seems to be most specific to the SPQ rather than the BAI, GHQ or AGE and is consistent with our results to H3 which isolate SPQ as a specific predictor of saccade amplitudes and tracking performance.

4 | DISCUSSION

Eye tracking has been used as a window into cognitive function since the early work of Yarbus (1967). In many of the paradigms which look at the tracking of moving targets, realism has been traded off for control and simplicity, often reducing tracked targets into points moving at constant speed along straight-line paths (Spering & Montagnini, 2011). That previous work has provided a range of insights and of particular relevance for the current study is the dynamics of pursuit responses from stimulus onset. Fast response latencies (~90–100 ms) lead to an open-loop stimulus-driven tracking initiation period (<200 ms) and then a closed-loop period where visual feedback mechanisms are expected to operate to maintain accurate tracking (Masson, 2004; Masson & Perrinet, 2012). The time course of performance in ocular tracking tasks has therefore previously been used to identify the hierarchical locus of motion processing computations (Pack & Born, 2001). In the current work, we sought to extend previous work by looking at tracking of motion trajectories which were more naturalistically curved by the effect of acceleration due to gravity. We had three questions of interest which motivated the hypotheses we tested.

4.1 | Can participants accurately track a naturalistically accelerating moving ball within a background with impoverished target depth and size cues?

We replicated previous work (Delle Monache, Lacquaniti, & Bosco, 2015; Jorges & Lopez-Moliner, 2019) finding that motion under gravity could be tracked very well and additionally showed that this could be done even with impoverished size and depth cues. We observed fast improvement up to a peak of performance for all participants within 150 ms (i.e. during the open loop) both for the gravity-influenced vertical and the horizontal components moving at a constant speed. This fast timescale is comparable to that previously measured under linear trajectories (Spering & Montagnini, 2011) and notably quicker than the 300 ms or so measured under curved arcs from a larger circle (Ross et al., 2017) or sinusoidal paths (Faiola et al., 2020; Meyhofer et al., 2015). It is also notably faster than motion tracking periods of up to 500 ms which were needed before participants could accurately compensate for a blanked trajectory of an accelerating target (Bennett et al., 2007), though that is notably a different task from tracking performance to identify individual differences. In the current work, motion in a gravitationally curved trajectory drove a tracking initiation with an appropriate acceleration comparable in performance dynamics to the simpler case of motion along a linear trajectory. This suggests specific adaptation to motion under gravity (Brenner et al., 2016; Jorges & Lopez-Moliner, 2017), and unlike previously thought, this may not require pictorial or context cues (Flavell, 2014; Zago et al., 2009). A recent study which included pictorial cues in the background of tracked parabola to support acceleration estimation tested a

range of values of gravity g from 0.7 to 1.3 (Jorges & Lopez-Moliner, 2019). Jorges and Lopez-Moliner (2019) found that gravity was tracked better than antigravity and there were large individual differences in this contrast between gravity conditions. For gravity tracking, we thought it interesting that they did not find the ecological value of $g = 9.81$ to be the best tracked motion in the range tested, though the authors acknowledge this may well have been because of confounds in the duration of the conditions with different values of g. If this effect is meaningful, it would support the notion that the system was flexible under different values of g and pictorial cues did not necessarily seem to engender optimal sensitivity to gravity. The current results provided evidence we interpret to suggest that the fast tracking dynamics comparable to straight-line tracking were likely to be driven by bottom-up sensory mechanisms during the initiation phase. This onset and timescale (100–150 ms) within the so-called open loop allow just enough time for a few sequential synapses in parallel to engage the fast network of midbrain structures, striate and extra-striate sensory visual cortex areas involved in motion processing and ocular responses (Masson & Perrinet, 2012). These early computations appear to be adapted for motion which follows the laws of physics.

4.2 | Will the inversion of gravity have a measurable effect on tracking?

Antigravity was processed much worse, with slower improvement to a plateau of performance for all participants, under all conditions. The dynamics suggest critical processing well into the closed-loop period (200–400 ms for the vertical direction compared to 200 ms for the constant horizontal speed direction) and make a case for a more complex, perhaps recurrent hierarchical computation. The advantage for the visual system which was identified for the motion under gravity was entirely lost under this inverted condition, consistent with previous results where deviations from g were tested during tasks involving interception (Zago et al., 2009). The current work supports the notion that gravity is in fact a special encoded feature, fundamentally impacting the way we perceive and operate in the world including seemingly unrelated aspects like aesthetic preferences and decision-making (Gallagher et al., 2019; Gallagher & Ferre, 2018). We conjecture that this fast stimulus processing case is similar to the high sensitivity to upright faces or light from above for which there is a quick, pre-attentive response along a similarly fast timescale to ecologically relevant stimuli (Rhodes, Brake, & Atkinson, 1993). In contrast, the atypical antigravity condition which would be analogous to the inverted faces cannot exploit the default sensory predictive mechanisms and so is performed worse for everyone engendering larger individual differences which we sought to understand further.

4.3 | Is there evidence that schizophrenia-associated trait levels have any link with individual performance and does this depend on the gravity conditions?

Dynamic predictive sensory and cognitive mechanisms incorporating experience may support the excellent tracking we observe under gravity (Fletcher & Frith, 2009; Jorges & Lopez-Moliner, 2019). These same mechanisms may not fully explain participant performance divergence and apparent compensation for the unexpected acceleration of inverted gravity seen in some participants. Corollary discharge signals (the neural signal produced in the brain to indicate actions performed by oneself) may have a role in how this pattern of results comes together and relates to schizotypy traits (Crapse & Sommer, 2008). We believe the time course of the antigravity result provides evidence of a hierarchical predictive computation which uses errors between efferent and afferent signals from an early sensory stage to adjust tracking online during the late part of the open-loop phase as it transitions to the closed loop, incorporating adjustments for expectations. It has been demonstrated that within such a framework, schizophrenic patients with impaired later stage prediction may be less sensitive to mathematical regularity or predictable structure in processing than healthy counterparts and may therefore improve when tracking unpredictable stimuli (Adams et al., 2012). We did not, however, measure an effect consistent with a better response to antigravity stimuli in the high-trait participants, perhaps because the inverted gravity condition in fact has a systematic regularity to it, just a less familiar acceleration rule providing the predictability than g. There was wide variability in performance which may be because some individuals (like sportspeople) might learn to expertly exploit laws of motion and harness predictive signals better than the rest of the population even in a novel context like antigravity. Conversely traits of neuropsychological conditions like schizophrenia might drive stronger tracking deficits when strong, possibly automatically processed, expectations like gravity are no longer helpful (Bansal et al., 2018). Recent work also established that orientation and motion illusions thought to be driven by strong ambiguity resolution assumptions or priors produced similar perceived illusions in both psychotic schizophrenic patients and healthy controls (Kaliuzhna et al., 2019). The similar tracking performance we observe across trait groups would support the notion that gravity is indeed a very strong prior acting for all participants including those with otherwise impaired predictive mechanisms (Jorges & Lopez-Moliner, 2017).

To test the prediction hypotheses, we established levels of individual traits using three self-report questionnaires, the specific Schizotypal Personality Questionnaire, SPQ (Raine, 1991), and as controls the General Health Questionnaire, GHQ (Hardy et al., 1999), and the Beck

Anxiety Inventory (Beck et al., 1988). While self-reports present some limitations in producing objective measures of trait and state, these established inventories have been shown to reliably capture the traits they seek to measure over previous studies, albeit with some individual variability (Fydrich et al., 1992; Hills et al., 2016; Hu et al., 2007). Our sample number ($N = 44$) was comparable to the lower end for which these inventories have previously been successfully used and splitting individuals into equal trait groups allowed us to visualise the dynamics of the changes across trait levels and test our third hypothesis. The SPQ was chosen to quantify schizotypy, a set of heterogenous traits found within the healthy population which are related to the positive, negative and disorganised symptoms of schizophrenia but which occur with a lower severity (Raine, 1991). Schizotypy, like schizophrenia, has consistently been shown to generate deficits in visual tracking (Faiola et al., 2020; Meyhofer et al., 2015; Spering et al., 2013). We therefore used the trait measure to split the participants into low and high groups and contrasted tracking performance between them. Results suggested that gravity-driven prediction mechanisms were active for both trait groups, consistent with previous findings of similar participant perception of visual illusions which rely on strong assumptions of the perceptual system (Kaliuzhna et al., 2019). Under the antigravity condition however, both groups were worse than under the gravity condition taking longer (200–400 ms) to attain stable tracking performance. The high-trait group performed worse than the low-trait group, starting from the same base at onset (implying that this was not simply due to poor fixation), but improving less quickly to reach a worse baseline of stable tracking performance. Both the tracking initiation and subsequent maintenance were poorer for the high SPQ trait group. As a control, we tested the GHQ and BAI traits in a similar way and found that negative scorers generated poorer tracking, with the entire dynamic tracking responses shifted upwards towards worse performance rather than replicating the shape of initiation and maintenance dynamics observed between the SPQ groups. In addition, the significant relationship between saccade size and SPQ score was not replicated across the control trait conditions. Using multivariate PCA, we identified five dominant component features within the data which explained over 99% of the variance. The first four of these components showed patterns that appeared to be related to (a) *negative mood* through SPQ and BAI (PC1), (b) *AGE*-dependent state (PC2), (c) *anxiety–schizotypy* related to the BAI and part of the SPQ (PC3) and (d) *positive mood* seen in the GHQ (PC4). The first two of these alone explained 85.3% of the variance in the data, and this was not unexpected as the behavioural traits and underlying neural mechanisms captured by these measures are known to show some overlap (Lewandowski et al., 2006; Samsom & Wong, 2015). The first four of these components had very small and inconsistent weightings for the eye movement metrics. We therefore assumed they predominantly captured comorbidity which could not be strongly associated with specific eye movements. It would be of interest to study these associations, further testing different forms of PCA (correlation-based and PCA regression) with larger sample sizes that allow for the decomposition of the SPQ into its constituent positive, negative and disorganised clusters and a similar decomposition of the GHQ into negative and positive.

The fifth component PC5 was dominated by eye-tracking performance, most importantly under the antigravity condition where variance weights were strongest. There was also a dynamic aspect to the patterns of these weights, suggesting different underlying processing for gravity and antigravity. In this light, PC5 appeared to specifically capture predictive performance divergence most strongly related to the earlier parts of the vertical RMSE and the saccade sizes in the antigravity condition. There was a specific significant relationship between these eye movement metrics and the SPQ in a way that was not seen in the control inventories, suggesting this SPQ-related prediction measure could be used to gather more insights from eye movements in future. These identified biometrics of prediction need to be explored further.

These findings demonstrated that our antigravity condition provided a window into dynamic tracking mechanisms specific to schizotypy. Imaging studies (fMRI) alongside tracking tasks have identified the networks that respond specifically to motion tracking including visual cortex, frontal areas, cerebellum and the thalamus, and of these, only sensory visual cortex showed a significantly higher activation for lower than for higher schizotypy groups during a tracking task (Meyhofer et al., 2015). Our findings of fast tracking dynamics support these results that gravity might obtain its fast processing advantage within appropriately adapted early sensory areas. Meyhofer and colleagues (2015) speculate that the non-significant trend towards higher activation in the frontal areas which is linked to schizotypy trait score might reflect a high-level compensatory mechanism applied by schizophrenic patients to deal with sensory–perceptual errors (Fletcher & Frith, 2009). Such a compensatory mechanism operating in frontal cortex would necessarily be slower than prediction processed at a sensory level by up to hundreds of milliseconds due to the recurrent hierarchical spiking computations that would need to be engaged to link the occipital lobe and the midbrain to the frontal networks (Thorpe, Fize, & Marlot, 1996). Further experiments need to be carried out to advance our understanding of the mechanistic underpinning of the heterogeneity in participants' performance we observe, a pattern of individual differences which has also similarly been shown to arise in a context-dependent way during visual motion ambiguity resolution (Li, Meso, Logothetis, & Keliris, 2019). It is also unclear whether the

capacity for implicit learning of the rules of motion during tracking shows any dependence on trait levels. A future question may be whether like primates (Bourrelly, Quinet, Cavanagh, & Goffart, 2016), some humans can eventually learn to track accelerating stimuli well, in our case specifically under antigravity over the course of many trials and what this says about the plasticity of dynamic brain function. There is also the question of whether schizophrenic patient tracking would be even more disrupted than our high schizotypy participants by the antigravity condition, and this should be tested.

5 | CONCLUSIONS

We have shown that human tracking of a ball which moves under the influence of gravity is performed very well, with fast reactions across all participants with a time course which reflects automated computations within the so-called open loop, while visual feedback remains limited and bottom-up sensory mechanisms are primarily active. In contrast, antigravity was generally poorly performed with longer delays before performance stabilised and resulted in a marked divergence in measured individual differences. We showed that while everyone performed well under the gravity condition, the antigravity condition produced better tracking for the low schizotypy trait participants who must have applied a compensatory mechanism for motion prediction in the closed-loop part of the response, which the high-trait individuals did not. This work provides a novel framework for studying sensorimotor prediction which we believe has a lot of potential and must be tested further. It also adds to a growing body of literature which provide encouraging early results in the quest for tools which can provide a diagnostic window into mechanisms of brain function (Faiola et al., 2020; Freedman & Foxe, 2018; Krol & Krol, 2019; Paladini et al., 2019), in our case dynamic prediction which can be an indication of psychotic traits.

ACKNOWLEDGEMENTS

We thank Bjorn Jorges for informative discussions about the gravity perception literature and Anna Montagnini and colleagues at the Institut de Neuroscience de la Timone in Marseille for critical comments which helped to improve the manuscript. We thank colleagues in the Visual Cognition Group at Bournemouth University for useful feedback during the project and Bournemouth University for financial support.

CONFLICT OF INTEREST

All authors—AIM, RDV, AM and PJH—confirm that there were no conflicts of interest to declare for this research project.

AUTHOR CONTRIBUTIONS

AIM, RDV, AM and PJH conceptualised the study. RDV, AM and AIM carried out the experiments and validated the collected data. AIM and PJH supervised the study. AIM developed the methodology, analysis tools, software and visualisations. AIM wrote the original draft. RDV, AM and PJH reviewed and edited the manuscript.

DATA AVAILABILITY STATEMENT

Data and analysis scripts will be available from the corresponding author upon reasonable request. The ultimate aim will be to make this and related subsequent data sets openly available after publication.

PEER REVIEW

The peer review history for this article is available at https://publons.com/publon/10.1111/ejn.14926

ORCID

Andrew Isaac Meso https://orcid.org/0000-0002-1919-7726
Peter J. Hills http://orcid.org/0000-0002-0097-9170

REFERENCES

Adams, R. A., Perrinet, L. U., & Friston, K. (2012). Smooth pursuit and visual occlusion: Active inference and oculomotor control in schizophrenia. *PLoS One*, *7*(10), e47502. https://doi.org/10.1371/journal.pone.0047502

Bansal, S., Ford, J. M., & Spering, M. (2018). The function and failure of sensory predictions. *Annals of the New York Academy of Sciences*, *1426*(1), 199–220. https://doi.org/10.1111/nyas.13686

Bargary, G., Bosten, J. M., Goodbourn, P. T., Lawrance-Owen, A. J., Hogg, R. E., & Mollon, J. D. (2017). Individual differences in human eye movements: An oculomotor signature? *Vision Research*, *141*, 157–169. S0042-6989(17)30039-1[pii]

Bates, D., Mächler, M., Bolker, B. M., & Walker, S. C. (2015). Fitting linear mixed-effects models using lme4. *Journal of Statistical Software*, *67*(1), 1–48. https://doi.org/10.18637/jss.v067.i01 .

Beck, A. T., Epstein, N., Brown, G., & Steer, R. A. (1988). An inventory for measuring clinical anxiety: Psychometric properties. *Journal of Consulting and Clinical Psychology*, *56*(6), 893–897. https://doi.org/10.1037//0022-006x.56.6.893.

Bennett, S. J., & Benguigui, N. (2013). Is acceleration used for ocular pursuit and spatial estimation during prediction motion? *PLoS One*, *8*(5), e63382. https://doi.org/10.1371/journal.pone.0063382.

Bennett, S. J., Orban de Xivry, J. J., Barnes, G. R., & Lefevre, P. (2007). Target acceleration can be extracted and represented within the predictive drive to ocular pursuit. *Journal of Neurophysiology*, *98*(3), 1405–1414. https://doi.org/10.1152/jn.00132.2007.

Bogadhi, A. R., Montagnini, A., & Masson, G. S. (2013). Dynamic interaction between retinal and extraretinal signals in motion integration for smooth pursuit. *Journal of Vision*, *13*(13), 5. https://doi.org/10.1167/13.13.5

Bonnet, C., Hanuska, J., Rusz, J., Rivaud-Pechoux, S., Sieger, T., Majerova, V., … Ruzicka, E. (2013). Horizontal and vertical eye movement metrics: What is important? [Clinical Trial Research

Support, Non-U.S. Gov't]. *Clinical Neurophysiology*, *124*(11), 2216–2229. https://doi.org/10.1016/j.clinph.2013.05.002

Bourrelly, C., Quinet, J., Cavanagh, P., & Goffart, L. (2016). Learning the trajectory of a moving visual target and evolution of its tracking in the monkey. *Journal of Neurophysiology*, *116*(6), 2739–2751. https://doi.org/10.1152/jn.00519.2016.

Brainard, D. H. (1997). The psychophysics toolbox. *Spatial Vision*, *10*(4), 433–436. https://doi.org/10.1163/156856897X00357

Brenner, E., Rodriguez, I. A., Munoz, V. E., Schootemeijer, S., Mahieu, Y., Veerkamp, K., … Smeets, J. B. J. (2016). How can people be so good at intercepting accelerating objects if they are so poor at visually judging acceleration? *i-Perception*, *7*(1), 204166951562431. https://doi.org/10.1177/2041669515624317

Brenner, E., Smeets, J. B. J., & de Lussanet, M. H. E. (1998). Hitting moving targets. Continuous control of acceleration of the hand on the basis of the target's velocity. *Experimental Brain Research*, *122*, 467–474. https://doi.org/10.1007/s002210050535

Bueno, A. P. A., Sato, J. R., & Hornberger, M. (2019). Eye tracking - The overlooked method to measure cognition in neurodegeneration? *Neuropsychologia*, *133*, 107191. https://doi.org/10.1016/j.neuropsychologia.2019.107191.

Casella, G., & Berger, R. L. (2002). *Statistical inference*, 2nd ed. Pacific Grove, CA: Brooks/Cole.

Crapse, T. B., & Sommer, M. A. (2008). Corollary discharge across the animal kingdom. *Nature Reviews Neuroscience*, *9*(8), 587–600. https://doi.org/10.1038/nrn2457.

Debono, K., Schutz, A. C., Spering, M., & Gegenfurtner, K. R. (2010). Receptive fields for smooth pursuit eye movements and motion perception. *Vision Research*, *50*(24), 2729–2739. https://doi.org/10.1016/j.visres.2010.09.034.

Delle Monache, S., Lacquaniti, F., & Bosco, G. (2015). Eye movements and manual interception of ballistic trajectories: Effects of law of motion perturbations and occlusions. *Experimental Brain Research*, *233*(2), 359–374. https://doi.org/10.1007/s00221-014-4120-9.

Diaz, G., Cooper, J., Rothkopf, C., & Hayhoe, M. (2013). Saccades to future ball location reveal memory-based prediction in a virtual-reality interception task. *Journal of Vision*, *13*(1), 20. https://doi.org/10.1167/13.1.20.

Engbert, R., & Kliegl, R. (2003). Microsaccades uncover the orientation of covert attention. *Vision Research*, *43*(9), 1035–1045. https://doi.org/10.1016/S0042-6989(03)00084-1.

Faiola, E., Meyhöfer, I., & Ettinger, U. (2020). Mechanisms of smooth pursuit eye movements in schizotypy. [Registered Report]. *Cortex*, *125*, 190–202. https://doi.org/10.1016/j.cortex.2019.12.008.

Flavell, J. C. A. (2014). *An investigation into the directional and amplitude aspects of an internal model of gravity*. Thesis (Ph.D.), Manchester Metropolitan University. Retrieved from http://hdl.handle.net/2173/336068.

Fletcher, P. C., & Frith, C. D. (2009). Perceiving is believing: A Bayesian approach to explaining the positive symptoms of schizophrenia. *Nature Reviews Neuroscience*, *10*(1), 48–58. https://doi.org/10.1038/nrn2536.

Freedman, E. G., & Foxe, J. J. (2018). Eye movements, sensorimotor adaptation and cerebellar-dependent learning in autism: Toward potential biomarkers and subphenotypes. *European Journal of Neuroscience 47*(6), 549–555. https://doi.org/10.1111/ejn.13625.

Fydrich, T., Dowdall, D., & Chambless, D. L. (1992). Reliability and validity of the beck anxiety inventory. *Journal of Anxiety Disorders*, *6*(1), 55–61. https://doi.org/10.1016/0887-6185(92)90026-4.

Gallagher, M., Arshad, I., & Ferrè, E. R. (2019). Gravity modulates behaviour control strategy. *Experimental Brain Research*, *237*(4), 989–994. https://doi.org/10.1007/s00221-019-05479-1.

Gallagher, M., & Ferre, E. R. (2018). The aesthetics of verticality: A gravitational contribution to aesthetic preference. *Quarterly Journal of Experimental Psychology (Hove)*, *71*(12), 2655–2664. https://doi.org/10.1177/1747021817751353.

Hardy, G. E., Shapiro, D. A., Haynes, C. E., & Rick, J. E. (1999). Validation of the general health questionnaire-12 using a sample of employees from England's health care services. *Psychological Assessment*, *11*(2), 159–165. https://doi.org/10.1037/1040-3590.11.2.159.

Hills, P. J., Eaton, E., & Pake, J. M. (2016). Correlations between psychometric schizotypy, scan path length, fixations on the eyes and face recognition. *Quarterly Journal of Experimental Psychology*, *69*(4), 611–625. https://doi.org/10.1080/17470218.2015.1034143.

Hosking, S. G., & Crassini, B. (2010). The effects of familiar size and object trajectories on time-to-contact judgements. *Experimental Brain Research*, *203*(3), 541–552. https://doi.org/10.1007/s00221-010-2258-7.

Hotelling, H. (1933). Analysis of a complex of statistical variables into principle components. *Journal of Educational Psychology*, *24*, 417–441, 498–520.

Hu, Y. J., Stewart-Brown, S., Twigg, L., & Weich, S. (2007). Can the 12-item General Health Questionnaire be used to measure positive mental health? *Psychological Medicine*, *37*(7), 1005–1013. https://doi.org/10.1017/S0033291707009993.

Ingster-Moati, I., Vaivre-Douret, L., Bui Quoc, E., Albuisson, E., Dufier, J. L., & Golse, B. (2009). Vertical and horizontal smooth pursuit eye movements in children: A neuro-developmental study. *European Journal of Paediatric Neurology*, *13*(4), 362–366. https://doi.org/10.1016/j.ejpn.2008.07.003.

Johannesson, O. I., Tagu, J., & Kristjansson, A. (2018). Asymmetries of the visual system and their influence on visual performance and oculomotor dynamics. *European Journal of Neuroscience*, *48*(11), 3426–3445. https://doi.org/10.1111/ejn.14225.

Jolliffe, I. T. (2002). *Principal component analysis*, 2nd ed. New York; London: Springer.

Jolliffe, I. T., & Cadima, J. (2016). Principal component analysis: A review and recent developments. *Philosophical Transactions of the Royal Society A: Mathematical, Physical and Engineering Sciences*, *374*(2065), 20150202. https://doi.org/10.1098/rsta.2015.0202.

Jorges, B., Hagenfeld, L., & Lopez-Moliner, J. (2018). The use of visual cues in gravity judgements on parabolic motion. *Vision Research*, *149*, 47–58. https://doi.org/10.1016/j.visres.2018.06.002.

Jorges, B., & Lopez-Moliner, J. (2017). Gravity as a strong prior: Implications for perception and action. *Frontiers in Human Neuroscience*, *11*, 1–16. https://doi.org/10.3389/fnhum.2017.00203.

Jorges, B., & Lopez-Moliner, J. (2019). Earth-gravity congruent motion facilitates ocular control for pursuit of parabolic trajectories. *Scientific Reports*, *9*(1), 14094. https://doi.org/10.1038/s41598-019-50512-6.

Kaliuzhna, M., Stein, T., Rusch, T., Sekutowicz, M., Sterzer, P., & Seymour, K. J. (2019). No evidence for abnormal priors in early vision in schizophrenia. *Schizophrenia Research*, *210*, 245–254. https://doi.org/10.1016/j.schres.2018.12.027.

Kim, I. K., & Spelke, E. S. (1992). Infants sensitivity to effects of gravity on visible object motion. *Journal of Experimental Psychology-Human Perception and Performance*, *18*(2), 385–393. https://doi.org/10.1037/0096-1523.18.2.385.

Kowler, E. (2011). Eye movements: The past 25 years. *Vision Research*, *51*(13), 1457–1483. https://doi.org/10.1016/j.visres.2010.12.014.

Krauzlis, R. J. (2003). Neuronal activity in the rostral superior colliculus related to the initiation of pursuit and saccadic eye movements. *The Journal of Neuroscience*, *23*(10), 4333–4344. https://doi.org/10.1523/JNEUROSCI.23-10-04333.2003

Krol, M. E., & Krol, M. (2019). A novel machine learning analysis of eye-tracking data reveals suboptimal visual information extraction from facial stimuli in individuals with autism. *Neuropsychologia*, *129*, 397–406. https://doi.org/10.1016/j.neuropsychologia.2019.04.022.

Land, M. F., & McLeod, P. (2000). From eye movements to actions: How batsmen hit the ball. *Nature Neuroscience*, *3*, 1340–1345. https://doi.org/10.1038/81887

Ledesma, R. D., & Valero-Mora, P. (2007). Determining the Number of Factors to Retain in EFA: An easy-to-use computer program for carrying out Parallel Analysis. *Practical Assessment Research & Evaluation*, *12*(2), 1–11.

Lee, E., Lee, J., & Kim, E. (2017). Excitation/inhibition imbalance in animal models of autism spectrum disorders. *Biological Psychiatry*, *81*(10), 838–847. https://doi.org/10.1016/j.biopsych.2016.05.011.

Lewandowski, K. E., Barrantes-Vidal, N., Nelson-Gray, R. O., Clancy, C., Kepley, H. O., & Kwapil, T. R. (2006). Anxiety and depression symptoms in psychometrically identified schizotypy. *Schizophrenia Research*, *83*(2–3), 225–235. https://doi.org/10.1016/j.schres.2005.11.024.

Li, Q., Meso, A. I., Logothetis, N. K., & Keliris, G. A. (2019). Scene regularity interacts with individual biases to modulate perceptual stability. *Frontiers in Neuroscience*, *13*, 523. https://doi.org/10.3389/fnins.2019.00523.

Mann, D. L., Nakamoto, H., Logt, N., Sikkink, L., & Brenner, E. (2019). Predictive eye movements when hitting a bouncing ball. *Journal of Vision*, *19*(14), 28. https://doi.org/10.1167/19.14.28.

Martinez-Conde, S., Otero-Millan, J., & Macknik, S. L. (2013). The impact of microsaccades on vision: Towards a unified theory of saccadic function. *Nature Reviews Neuroscience*, *14*(2), 83–96. https://doi.org/10.1038/nrn3405.

Masson, G. S. (2004). From 1D to 2D via 3D: Dynamics of surface motion segmentation for ocular tracking in primates. *Journal of Physiology-Paris*, *98*(1–3), 35–52. https://doi.org/10.1016/j.jphysparis.2004.03.017

Masson, G. S., & Perrinet, L. U. (2012). The behavioral receptive field underlying motion integration for primate tracking eye movements. *Neuroscience & Biobehavioral Reviews*, *36*(1), 1–25. https://doi.org/10.1016/j.neubiorev.2011.03.009

Medathati, N. V. K., Rankin, J., Meso, A. I., Kornprobst, P., & Masson, G. S. (2017). Recurrent network dynamics reconciles visual motion segmentation and integration. *Scientific Reports*, *7*, 1–15. https://doi.org/10.1038/s41598-017-11373-z.

Meso, A. I., Montagnini, A., Bell, J., & Masson, G. S. (2016). Looking for symmetry: Fixational eye movements are biased by image mirror symmetry. *Journal of Neurophysiology*, *116*(3), 1250–1260. https://doi.org/10.1152/jn.01152.2015.

Meso, A. I., Rankin, J., Faugeras, O., Kornprobst, P., & Masson, G. S. (2016). The relative contribution of noise and adaptation to competition during tri-stable motion perception. *Journal of Vision*, *16*(15), 6. https://doi.org/10.1167/16.15.6

Meyhofer, I., Steffens, M., Kasparbauer, A., Grant, P., Weber, B., & Ettinger, U. (2015). Neural mechanisms of smooth pursuit eye movements in schizotypy. *Human Brain Mapping*, *36*(1), 340–353. https://doi.org/10.1002/hbm.22632.

Mijatovic, A., La Scaleia, B., Mercuri, N., Lacquaniti, F., & Zago, M. (2014). Familiar trajectories facilitate the interpretation of physical forces when intercepting a moving target. *Experimental Brain Research*, *232*(12), 3803–3811. https://doi.org/10.1007/s00221-014-4050-6.

Murray, J. D., Anticevic, A., Gancsos, M., Ichinose, M., Corlett, P. R., Krystal, J. H., & Wang, X. J. (2014). Linking microcircuit dysfunction to cognitive impairment: Effects of disinhibition associated with schizophrenia in a cortical working memory model. *Cerebral Cortex*, *24*(4), 859–872. https://doi.org/10.1093/cercor/bhs370.

Myles, J. B., Rossell, S. L., Phillipou, A., Thomas, E., & Gurvich, C. (2017). Insights to the schizophrenia continuum: A systematic review of saccadic eye movements in schizotypy and biological relatives of schizophrenia patients. [Review Research Support, Non-U.S. Gov't]. *Neuroscience & Biobehavioral Reviews*, *72*, 278–300. https://doi.org/10.1016/j.neubiorev.2016.10.034.

Orban de Xivry, J. J., Coppe, S., Blohm, G., & Lefevre, P. (2013). Kalman filtering naturally accounts for visually guided and predictive smooth pursuit dynamics. *Journal of Neuroscience*, *33*(44), 17301–17313. https://doi.org/10.1523/JNEUROSCI.2321-13.2013.

Orban de Xivry, J. J., & Lefevre, P. (2007). Saccades and pursuit: Two outcomes of a single sensorimotor process. [Research Support, Non-U.S. Gov't Review]. *The Journal of Physiology*, *584*(Pt 1), 11–23. https://doi.org/10.1113/jphysiol.2007.139881.

Pack, C., & Born, R. T. (2001). Temporal dynamics of a neural solution to the aperture problem in visual area MT of macaque brain. *Nature*, *409*, 1040–1042. https://doi.org/10.1038/35059085

Paladini, R. E., Wyss, P., Kaufmann, B. C., Urwyler, P., Nef, T., Cazzoli, D., … Muri, R. M. (2019). Re-fixation and perseveration patterns in neglect patients during free visual exploration. *European Journal of Neuroscience*, *49*(10), 1244–1253. https://doi.org/10.1111/ejn.14309.

Pearson, K. (1901). On Lines and Planes of Closest Fit to Systems of Points in Space. *Philosophical Magazine*, *6*(2), 559–572.

Pelli, D. G. (1997). The VideoToolbox software for visual psychophysics: Transforming numbers into movies. *Spatial Vision*, *10*(4), 437–442. https://doi.org/10.1163/156856897X00366

Raine, A. (1991). The SPQ - a scale for the assessment of schizotypal personality based on DSM-III-R Criteria. *Schizophrenia Bulletin*, *17*(4), 555–564. https://doi.org/10.1093/schbul/17.4.555.

R-Core-Team. (2019). *R: A langauge and environment for statistical computing*. Vienna, Austria: R Foundation for Statistical computing.

Rhodes, G., Brake, S., & Atkinson, A. P. (1993). Whats lost in inverted faces. *Cognition*, *47*(1), 25–57. https://doi.org/10.1016/0010-0277(93)90061-Y.

Ross, N. M., Goettker, A., Schutz, A. C., Braun, D. I., & Gegenfurtner, K. R. (2017). Discrimination of curvature from motion during smooth pursuit eye movements and fixation. *Journal of Neurophysiology*, *118*(3), 1762–1774. https://doi.org/10.1152/jn.00324.2017.

Rottach, K. G., Zivotofsky, A. Z., Das, V. E., AverbuchHeller, L., Discenna, A. O., Poonyathalang, A., & Leigh, R. J. (1996). Comparison of horizontal, vertical and diagonal smooth pursuit eye movements in normal human subjects. *Vision Research*, *36*(14), 2189–2195. https://doi.org/10.1016/0042-6989(95)00302-9.

Rucci, M., & Victor, J. D. (2015). The unsteady eye: An information-processing stage, not a bug. *Trends in Neuroscience*, *38*(4), 195–206. https://doi.org/10.1016/j.tins.2015.01.005.

Samsom, J. N., & Wong, A. H. (2015). Schizophrenia and depression co-morbidity: What we have learned from animal models. *Frontiers in Psychiatry*, *6*, 13. https://doi.org/10.3389/fpsyt.2015.00013.

Spering, M., Dias, E. C., Sanchez, J. L., Schutz, A. C., & Javitt, D. C. (2013). Efference copy failure during smooth pursuit eye movements in schizophrenia. *Journal of Neuroscience*, *33*(29), 11779–11787. https://doi.org/10.1523/Jneurosci.0578-13.2013.

Spering, M., & Montagnini, A. (2011). Do we track what we see? Common versus independent processing for motion perception and smooth pursuit eye movements: A review. *Vision Research*, *51*(8), 836–852. https://doi.org/10.1016/j.visres.2010.10.017

Thorpe, S., Fize, D., & Marlot, C. (1996). Speed of processing in the human visual system. *Nature*, *381*(6582), 520–522. https://doi.org/10.1038/381520a0.

Wegner-Clemens, K., Rennig, J., Magnotti, J. F., & Beauchamp, M. S. (2019). Using principal component analysis to characterize eye movement fixation patterns during face viewing. *Journal of Vision*, *19*(13), 2. https://doi.org/10.1167/19.13.2.

Werkhoven, P., Snippe, H. P., & Toet, A. (1992). Visual processing of optic acceleration. *Vision Research*, *32*(12), 2313–2329. https://doi.org/10.1016/0042-6989(92)90095-Z.

Xiao, J. B., & Huang, X. (2015). Distributed and dynamic neural encoding of multiple motion directions of transparently moving stimuli in cortical area MT. *Journal of Neuroscience*, *35*(49), 16180–16198. https://doi.org/10.1523/Jneurosci.2175-15.2015.

Yarbus, A. L. (1967). *Eye movements and vision*. New York, NY: Plenum Press.

Young, H. D. A., Freedman, R. A. A., and Ford, A. L. A. (2011). *University physics with modern physics* (13 edn). Boston, MA: Addison-Wesley.

Zago, M., McIntyre, J., Senot, P., & Lacquaniti, F. (2009). Visuo-motor coordination and internal models for object interception. *Experimental Brain Research*, *192*(4), 571–604. https://doi.org/10.1007/s00221-008-1691-3.

How to cite this article: Isaac Meso A, De Vai RL, Mahabeer A, Hills PJ. Evidence of inverted gravity-driven variation in predictive sensorimotor function. *Eur J Neurosci*. 2020;52:4803–4823. https://doi.org/10.1111/ejn.14926